NASA CR-54965

FINAL REPORT
ON
DEVELOPMENT OF OPTICAL COATINGS
FOR
CdS THIN FILM SOLAR CELLS

By

J. C. SCHAEFER, E. R. HILL

Prepared For

NATIONAL AERONAUTICS AND SPACE ADMINISTRATION

CONTRACT NAS3-6464

THE HARSHAW CHEMICAL CO.

N O T I C E

This report was prepared as an account of Government sponsored work. Neither the United States, nor the National Aeronautics and Space Administration (NASA), nor any person acting on behalf of NASA:

A.) Makes any warranty or representation, expressed or implied, with respect to the accuracy, completeness, or usefulness of the information contained in this report, or that the use of any information, apparatus, method, or process disclosed in this report may not infringe privately owned rights; or

B.) Assumes any liabilities with respect to the use of, or for damages resulting from the use of any information, apparatus, method, or process disclosed in this report.

As used above, "person acting on behalf of NASA" includes any employee or contractor of NASA, or employee of such contractor, to the extent that such contractor prepares, disseminates, or provides access to, any information pursuant to his employment or contract with NASA, or his employment with such contractor.

Requests for copies of this report should be referred to:

National Aeronautics and Space Administration
Office of Scientific and Technical Information
Attention: AFSS-A
Washington, D.C. 20546

NASA CR 54965

Final Report

Optical Coatings For CdS Photovoltaic Film Cells

by

E. R. Hill and J. C. Schaefer

Prepared For

National Aeronautics and Space Administration

December 1965

Contract NAS3-6464

Abstract

Investigation was conducted on the optical properties of high infrared emittance optical films deposited on CdS solar cells. Materials were selected and deposited by sputtering and thermal evaporation. Measurements were made of emittance and cell stability in humid atmosphere.

Foreword

This report was prepared by the Crystal-Solid State Division of The Harshaw Chemical Company. The work was sponsored by the Space Power Systems Procurement Section of the NASA, Lewis Research Center with Dr. A. E. Potter acting as Technical Advisor and Mr. Clifford Swartz as Project Manager.

During this contract Dr. J. McKenzie was Technical Director of the Crystal Solid State Laboratory of The Harshaw Chemical Company. Project Direction was provided by Mr. J. C. Schaefer with Mr. E. R. Hill as Project Leader. The following Harshaw personnel contributed to this program; R. W. Olmsted, R. J. Humrick, W. W. Baldauf, and D. J. Krus.

Table of Contents

List of Illustrations

List of Tables

Summary

Suitable materials were chosen for deposition in film form onto CdS solar cells. The criteria included infrared optical properties, and chemical and mechanical stability. The materials selected were $CaCO_3$, Al_2O_3, SiO_2 and MgF_2. Sputtering and thermal evaporation were investigated as means for deposition of the films. Sputtering was found to be too delicate and too slow to be feasible as a production process. MgF_2 and SiO were thermally evaporated and the resulting films analyzed. Measurements were made of emittance of the CdS cell both bare and with various coatings. Cells with various coatings were stored in a humid environment and performance measured. The combination of 1/3 micron of SiO_x overlayed with 3 to 10 microns of MgF_2 appeared most promising.

Introduction

The purpose of this program has been to develop and apply optical coatings to CdS solar cells to obtain an increase in the solar power conversion efficiency and to obtain a degree of protection against moisture damage. It is desired to maximize the amount of light entering the cell in the region of spectral sensitivity, reflect as much as possible of all others, and to maintain a low operating temperature in extraterrestrial space. These conditions are not all independent. For example, a metallic surface which absorbs strongly will also be a good reflector and consequently a poor emitter. The parameters for the problem are as follows. The cell responds to all wavelengths less than about 1 micron. The sun is approximately a 6000°K black body. It is assumed that the cell receives sunlight at normal incidence and reradiates to empty space. These conditions determine the desired optical properties of the cell. Further, it is necessary that the applied coatings be mechanically and chemically stable in terrestrial and extraterrestrial environments. This implies that the coating protect the cell from water vapor at sea level and be stable under radiation in the van Allen belt. These requirements are relatively restrictive and limit the materials which can be used effectively.

Optical Properties Of Cell and Coating

The main requirements for the cell coating are that it be transparent to wavelengths of light less than 1 micron and have high emittance for wavelengths emitted by the cell at its steady state operating temperature. The cell itself has an index of refraction about 2.5, so to reduce reflection losses, the coating should have an index around 1.5 to 1.6. The p-type layer on the CdS cell has a high infrared reflectance and a low emittance of about 0.2. The material sought for the coating should have an emittance of 0.7 to 0.8.

A wide variety of materials are available which are visibly transparent and have a refractive index in the range near 1.5. The property of high emittance narrows the field. For calculation purposes, it is assumed that the cell absorbs all the solar radiation and must reradiate 90% back to empty space. A black body under these conditions comes to a steady state temperature of about 333°K. Consequently, the coating must have high emittance for those wavelengths emitted by a 333°K black body. Figure 1 shows the spectral distribution of radiation from such a source, with Figure 2 showing the integrated curve. As can be seen, most of the power is emitted in the band between 5 and 25 microns, so it is in this band that the emittance must be high.

A compromise must be made in the case of material in film form. To obtain high emittance, the absorptance must be high and reflectance low. However, to reach high absorptance in a film,

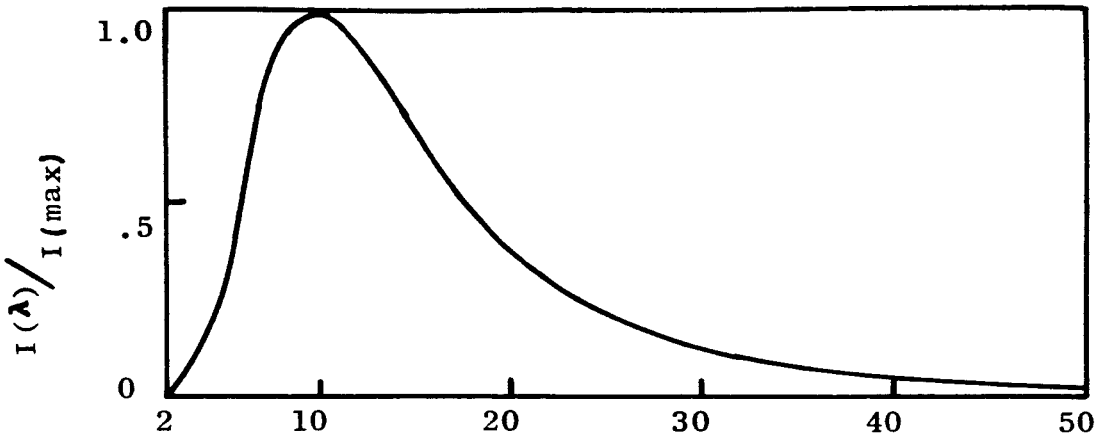

Spectral Irradiance of 333°K Black Body

Figure 1

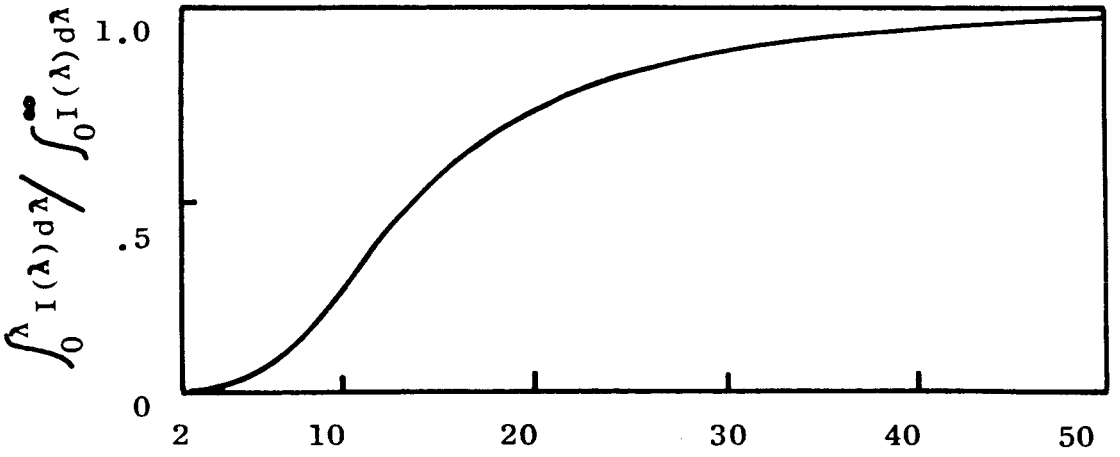

Integrated Spectral Irradiance of

333°K Black Body

Figure 2

the absorption coefficient must be high. This automatically makes for high reflectance. Thus, the compromise is to have a moderately thick film with a moderate absorption coefficient. For emittances above 0.5, this implies films 3 to 10 microns thick with absorption coefficients between 10^3 and 10^4 cm^{-1} in the range between 5 and 25 micron wavelength.

Optical absorption in this wavelength range in solids is associated with vibrations of the ions in the lattice excited by the incident light. A simple picture of this is found in Kittel's "Introduction to Solid State Physics"(1). From Kittel, the amplitude of vibration induced in a diatomic molecular chain is:

$$d = \frac{A}{w_o^2 - w^2}$$

d = displacement of the ion

A = constant containing ionic mass and the forcing amplitude

w = frequency of the incident light (frequency of the force applied)

w_o = natural frequency of the lattice

$w_o^2 = \beta\left(\frac{1}{M} + \frac{1}{m}\right)$

β = spring constant between ions

M,m = ionic masses

In terms of wavelengths, this becomes

$$d = \frac{A}{c^2} \frac{(\lambda_o^2 \lambda^2)}{(\lambda_o^2 - \lambda^2}$$

where c = velocity of light

$$\lambda_o = \frac{c}{w_o}$$

$$\lambda = \frac{c}{w}$$

The absorption of the incident light will be large when the induced vibration is large and so the absorption will be decreasing at longer and shorter wavelengths. The high absorption will be very large at $\lambda = \lambda_o$, decreasing at longer and shorter wavelengths. The high absorption at $\lambda = \lambda_o$ produces metallic reflection and is known as Restrahlen. As the absorption decreases, so will the reflectance. The range of interest for this application will be that on the short wavelength side of the Restrahlen where the absorption coefficient ranges from 10^3 to 10^4 cm^{-1}. In general, all solids will have the same variation of absorption with wavelength and the materials for this application will be those with Restrahlen wavelengths beyond 20 microns and moderate absorbance to about 5 microns. Figure 3 shows the absorbance and reflectance spectra for some of the better known candidate materials. The uniformity of character shows up clearly and the nature of the compromise to be made is easily seen. Those materials which are opaque to shorter wavelengths also have high reflectance at shorter wavelength. The gap between these two regions is that which is to be fitted to the spectrum of radiation from the 333°K black body. The materials best meeting this requirement are $CaCO_3$, SiO_2, LiF, MgF_2, CaF_2, BaF_2, and Al_2O_3.

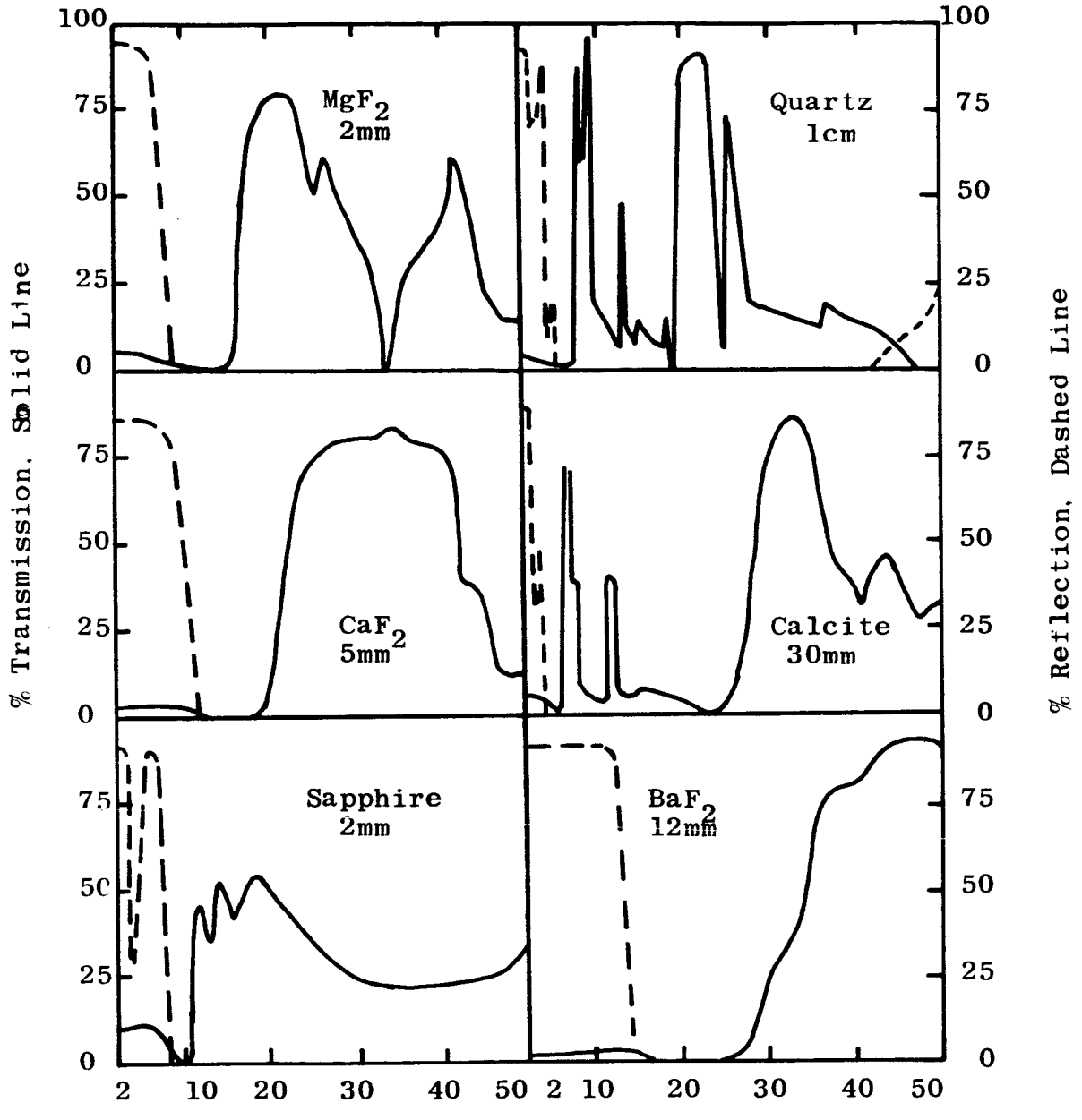

Transmission and Reflection Spectra For

Various Dielectrics*

Figure 3

* The Reflection and Transmission of Infrared Materials; McCarthy, D.E. Applied Optics, Vol. 4, #3, March 65, p. 317 and Vol. 2, #6, June 63, p. 591

Thin Film Properties

As noted in the previous discussion, high emittance is most easily attained by a thick layer of material with a moderate absorption coefficient. By the nature of the product, the layer on the CdS solar cell must be a thin film and be applied to cells 3 inches square. To retain the concept of a light-weight, flexible cell, the coating should be no more than 10 microns thick and be mechanically flexible. To achieve this, the coating can be deposited by sputtering, or vacuum evaporation, or painting.

Plastics which can be painted on or laminated onto the surface of the cell generally have undesirable infrared optical properties. The most promising would be the silicone resins which have some of the absorption characteristics of glass.

Films of MgF_2 and glass which are deposited by evaporation and sputtering have the desired optical characteristics. However, in layers over 1 micron in thickness, the residual stresses developed during deposition cause mechanical instability in the form of peeling or checking of the film. While checking may not destroy the optical properties, the usefulness of the film as a moisture barrier is lost. Previously, it has been found that 1/3 micron of SiO evaporated onto the cell greatly reduced the water vapor attack. Consequently, a two layer evaporated film was attempted. Glass or SiO was first deposited to a thickness of 1000 to 3000 Å and over this a thick layer of MgF_2 was vacuum deposited. Results for this are shown in the section on measurements.

Material Properties

The optical requirements for the coating material have limited the number of materials which are likely candidates to seven. These are $CaCO_3$, SiO_2, LiF, MgF_2, CaF_2, BaF_2 and Al_2O_3. BaF_2 and CaF_2 are slightly water soluble and are not particularly hard in the film form. They would be marginally useful. LiF is composed of relatively light ions and does suffer damage in the van Allen belt. This reduces the list to $CaCO_3$, Al_2O_3, SiO_2, and MgF_2. The first two materials are highly refractory and decompose when heated in a vacuum. In the molten state, they also react with materials which could be used as crucibles. Thus Al_2O_3 and $CaCO_3$ must be either sputtered or evaporated by electron beam heating. SiO_2 and MgF_2 can also be deposited in these ways. Furthermore, SiO can be evaporated from most refractory metal crucibles to form films of SiO_x. MgF_2 can also be vacuum evaporated from most metal boats.

As a consequence of the properties discussed, the course of this program was to pursue the sputtering of Al_2O_3 and SiO_2 in the attempt to develop a process where these materials could be deposited in the required thickness in a reasonable time period. Also, MgF_2 was vacuum evaporated with the aim to deposit thick continuous films onto a relatively cool substrate.

Organic coatings in the form of sheet plastics and paints were also investigated. The infrared absorption spectra of these materials show strong bands which are usually quite narrow. The most promising are the silicone resins and coatings

of silicone varnishes. The normal laminating plastics were also investigated.

Methods of Coating

Evaporation

The preparation of thin films by the technique of vacuum evaporation is a standard process for producing anti-reflection coatings on lenses and complex multi-layer interference filters. Most materials do not evaporate and condense congruently, but the simplicity of the method itself suggests that it be attempted where possible. Examples of materials which can be evaporated are: SiO, MgF_2, CaF_2, and LiF. Although evaporation of the aforementioned materials is possible, not all are achieved with the same ease nor are the results for each material the most desirable. The vacuum evaporation apparatus which was used for experiments with the various materials was a Kinney High Vacuum Evaporator, Model SC-3. The layout of the substrate holder, resistance heated boats, substrate heater is shown in Figure 4. The resistance heated boats would be considered as a direct surface source and evaporations are assumed to take place according to Knudsen's calculations. The equation for calculation of thickness of deposited films at a point directly above the source would be:

$$t = \frac{m}{\pi \rho} \cdot \frac{1}{h^2}$$

where m = mass evaporation

ρ = density of material

h = distance from source to substrate

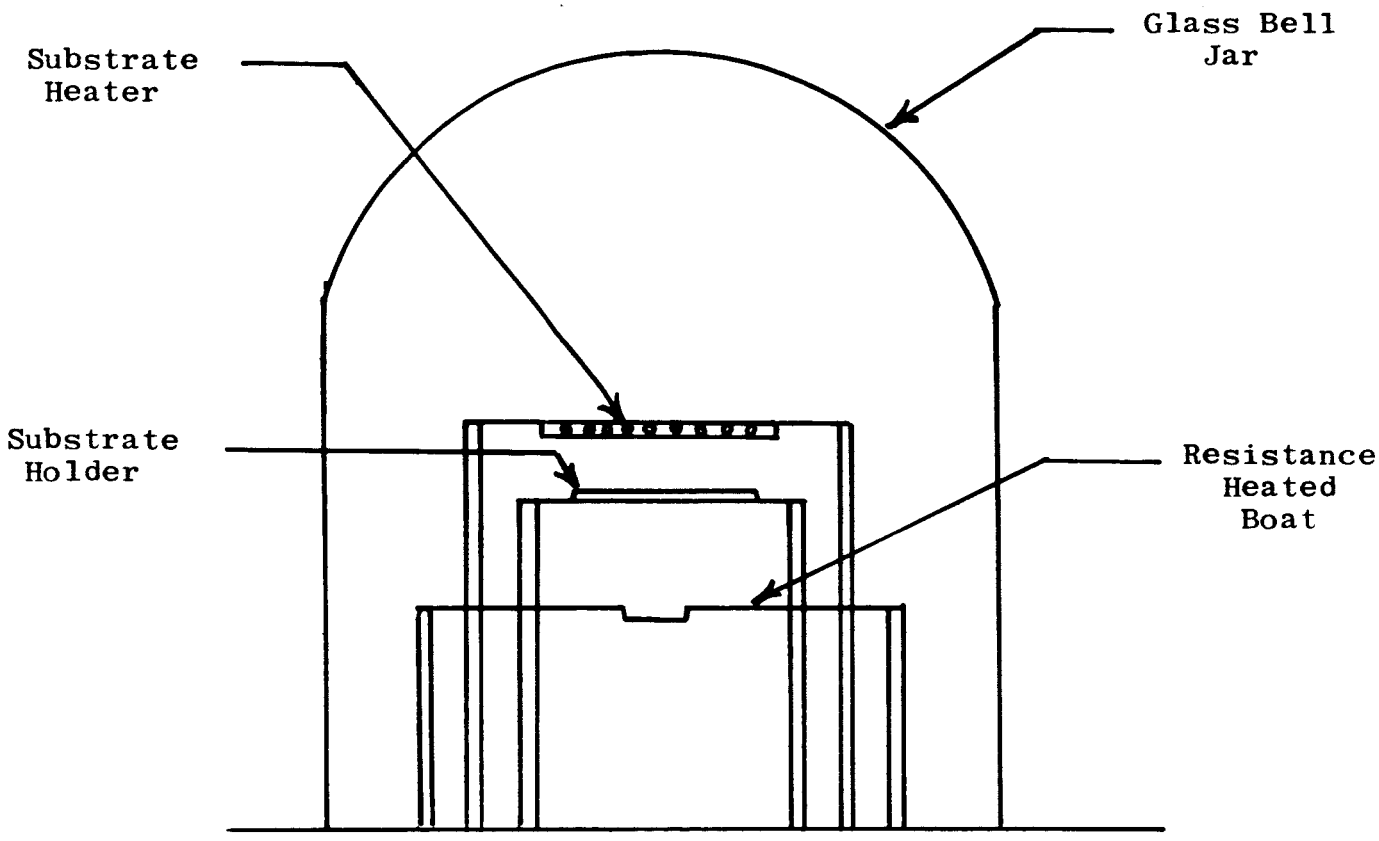

Vacuum Evaporation Set-Up

Figure 4

The evaporation rate can be vitally important in the formation of optical films by the vacuum evaporation method and varies from one type of material to another. Generally, it can be said that higher rates are more conductive to good optical films with the exception of SiO in which pinholes are reduced by use of low deposition rates.

Stresses are formed in deposited films and indications are that as the film thickness increases, the stress also increases. This is partly due to the temperature gradient through the deposit and the substrate. Another important factor is the increase in crystallite size as the film grows. Elevated substrate temperatures generally produce films with lower residual stress. Even at higher substrate temperatures, stresses will be induced due to expansion coefficients differing as well as other property differences of the substrate and the material being deposited. Initial evaporation of SiO and MgF_2 were accomplished at pressures of 2×10^{-5} mm Hg on substrates at room temperatures. Rates of evaporation were relatively low, in the 30 to 100 Å per second range. Almost invariably the films that were of any reasonable thickness were mechanically unstable. Generally the films would peel from the substrate without any outside influence and those apparently adhering were easily flaked off by a minor amount of flexing of the substrate. Both SiO and MgF_2 evaporations were similar in results when thicker coatings (>1.0 microns) were fabricated under the above conditions.

In order to improve the adhesion of the coating, a substrate heater was installed in the vacuum evaporator. The temperature of the substrate was raised to approximately 60°C for deposition experiments. At this temperature, with the other parameters remaining the same, erratic results were also obtained for deposits of one micron or more. Some films were made on which the coating had very good adhesion and others which immediately on removal from the chamber commenced flaking off. When the films that appeared to have adequate adhesion were viewed under magnification it could be seen that there were still some discontinuities in the coating.

Further improvement in the adhesion of the coating was accomplished by raising the substrate temperature to 270-300°C, and increasing the deposition rate to 250 Å per second. Using this procedure, good adhering films over the range from three to eight microns thick were produced.

Table I lists a number of evaporations of various materials and the results that were obtained. A number of coated cells were sent to NASA for evaluation and are listed in Table II.

Sputtering-Film Deposition

Procedures

Film deposition by sputtering is a well-known process and has been adequately described in the literature. Dielectric sputtering using the R-F plasma triode system was developed by Wehner[2] and his co-workers and they have investigated the process using many different materials. This technique was

Table I

Results of Coating Evaporations

No. of Evaps.	Material for Evaporations	Evaporations Substrate	Source Temp.	Substrate Temp.	Thickness	Mechanical Stability
2	MgF_2	Moly	1500°	Ambient	3	Large flakey crystals
3	MgF_2	CdS Cell	1500°	Ambient	8-10,000 Å	Fair
2	MgF_2	Aluminum	1500°	Ambient	6,000 Å	Good film
2	MgF_2	Aluminum	1500°	Ambient	1.5-2.0	Poor
1	MgF_2	Aluminum	1500°	Ambient	4.0	Very poor
2	CaF_2	CdS Cell	1400°	60°C	2.0-3.0	Poor
4	SiO	CdS Cell	1300°	60°C	1.0	Good
6	MgF_2	CdS Cell	1500°	60°C	2.0-3.0	Fair
15	MgF_2	CdS Cell	1500°	250°C	2.0	Fair to Good
4	SiO-MgF_2	CdS Cell	1300° & 1500°	250°C	.5 SiO 2.0 MgF_2	Fair
2	MgF_2	CdS Cell	1500°	250°C	8.0	Good

Table II

Sample Cells Delivered To NASA

Cell No.	Area	Eff.(After coating & Lamination)
1	2.3 cm^2	3.4%
2	2.3 cm^2	3.7%
3	2.3 cm^2	3.0%
4	2.3 cm^2	2.8%
5	2.3 cm^2	3.0%
170	2.3 cm^2	3.2%
10	2.1 cm^2	2.8%
11	2.1 cm^2	3.1%
2-1	2.1 cm^2	2.7%
3-3	2.0 cm^2	2.8%

chosen as one approach for this program because any dielectric which can be made into a suitable shape can be sputtered. The particular aim was to deposit 3 to 10 microns thick layers of glass onto the CdS cell at a rate of 0.1 to 1 micron per minute without adversely affecting the cell. Once the process was developed for glass, other insulators such as alumina and calcite could be studied.

The equipment used was fabricated from the CVC AST100 sputtering system and the necessary R-F generator and amplifier. Schematic diagrams of the apparatus are shown in Figures 5 and 6. In principle, the system simply couples an R-F power source to a capacitor formed by the target electrode, glass target and the plasma column. Power is dissipated in the glass target by the positive ions on collision with the glass. Most of this power appears as Joule heating of the glass with the remainder carried away by the sputtered material.

After a period of trial and error in becoming acquainted with the system, glass films were sputtered and data taken on performance. Tables III and IV show typical rate data for sputtering of pyrex glass in Argon gas. Noteworthy features are as follows: First, sputtering takes place at a pressure of about 0.5 microns of Hg where the mean free path is 10 cm. A target-substrate spacing of 5 cm results in 40% of the sputtered material being scattered before reaching the substrate. This is a significant improvement over two electrode diode sputtering where the pressure would be at least 10 microns of Hg and about 87% of the sputtered material would be scattered before reaching the substrate. Secondly, the deposition rate is quite low, at

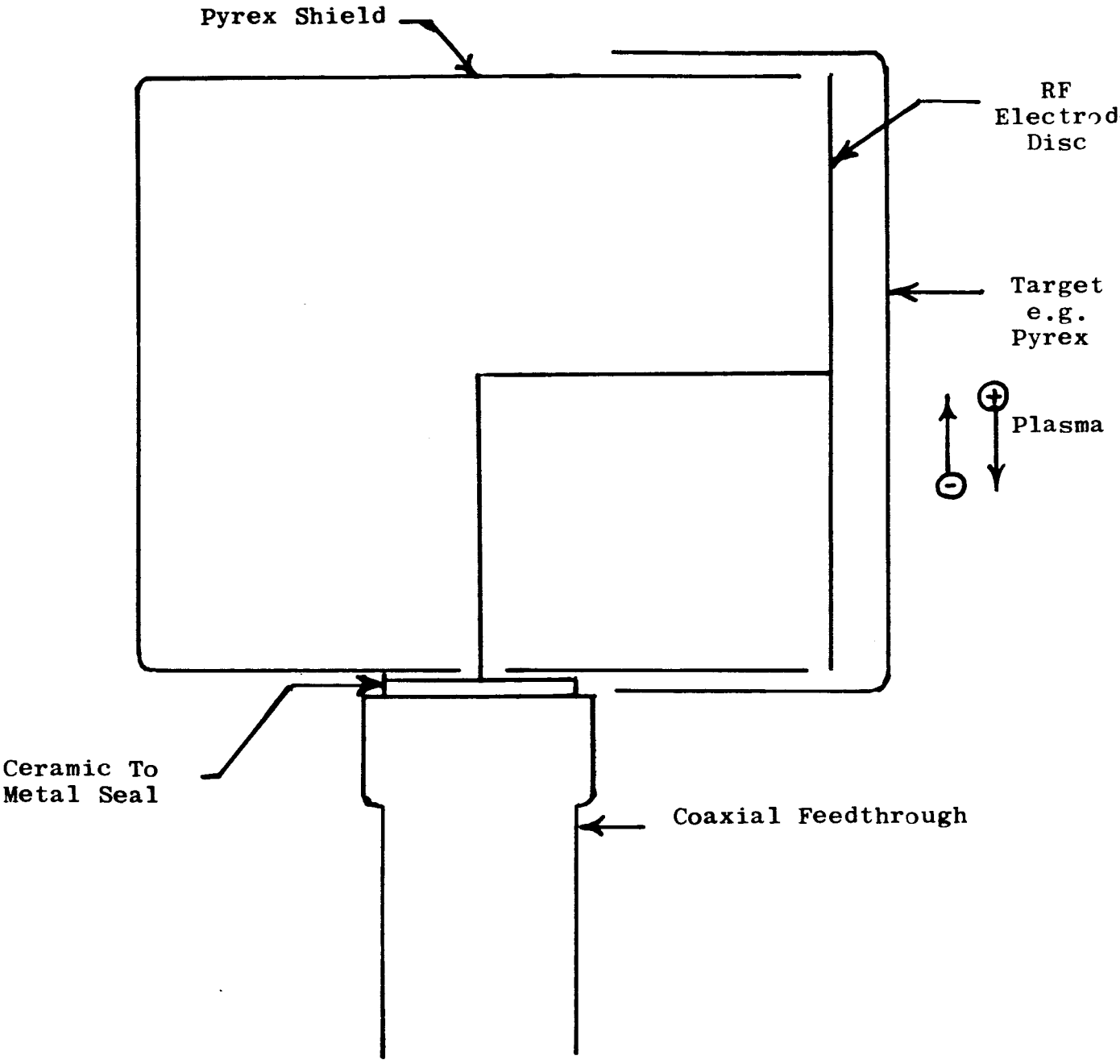

Schematic Diagram Of RF Probe

Figure 5

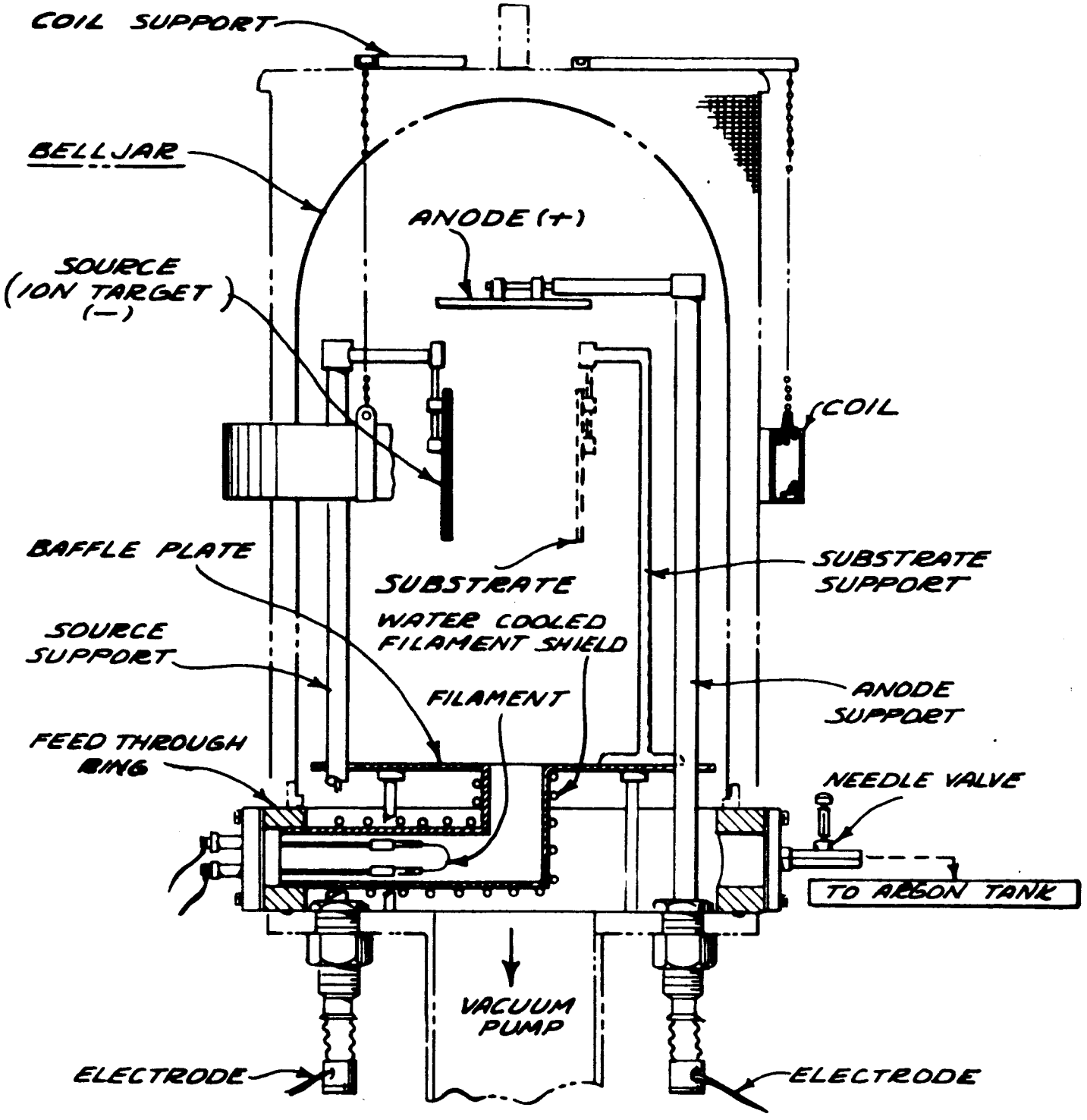

Schematic Diagram of Sputtering Apparatus

Figure 6

Table III

Sputtered Pyrex Coatings on Small Areas

Pressure Gauge (μ Hg)	Net RF Power (Watts)	Target Electrode Area (cm^2)	Deposition Rate (μ/hr)	Remarks
10.0	200	16	0.02	Thickness from Angstrometer
3.0	130	16	0.1	Thickness from Angstrometer
3.0	175	16	0.015	Thickness from Angstrometer
0.5	320	79	0.24	Thickness from Sample Weight
0.65	320	79	0.5	Thickness from Sample Weight
0.5	330	79	0.38	Thickness from Sample Weight
0.65	317	79	0.51	Thickness from Sample Weight

Note:

Argon gas ambient.

Pyrex crystallization dishes were used as targets.

The samples used for the thickness determination by weight were approximately 2 cm x 3.5 cm.

Table IV

Sputtered Pyrex Coatings on Large Areas

Pressure Gauge (μ Hg)	Net RF Power (Watts)	Substrate Thermometer (°C)	Deposition Rate (μ/hr)
0.52	335		0.25
0.53	340	300	0.25
0.50	400	233	0.27
0.55	390	208	0.27
0.55	320	234	0.36

Note:

Argon gas ambient.

Pyrex crystallization dishes were used as targets;

Electrode area: 79 cm^2.

The samples were approximately 7 cm x 3.5 cm.

The average deposition rate over these larger area samples was about half what it was on the smaller samples.

The main advantage expected to be gained by sputtering of a dielectric is that the composition of the deposited layer will be very nearly that of the parent material. In otherwords, the material should be removed and deposited congruently. It was hoped that this would evidence itself in lower residual stresses and eliminate peeling of the deposited film. There was no clear-cut evidence that this was the case when glass is sputtered in Argon. Films over 1 micron thick were about as stable as those made by thermal evaporation of SiO. The addition of 40% oxygen to the sputtering gas did eliminate the problem of peeling. However, the sputtering rate was also reduced, as is shown in Table V.

Sputtering-Conclusions

From the data gathered on the sputtering investigation, qualitative and quantitative conclusions can be drawn. The first is concerning the usefulness of the system itself. For the purposes desired in this program, the system is extremely delicate to operate. At the power levels required, the system is inherently unstable due to the negative resistivity temperature coefficient of insulators and catastrophic failures can result. Aside from this, the mechanics of transmission of power to the target are difficult to carry out inside the evacuated bell jar.

Quantitatively, from the data obtained, the temperature of the substrate can be predicted from a knowledge of the deposition rate. Our experiments gave, at best, one molecule for about ten thousand electron volts of energy. Recently disclosed findings by P. D. Davidse and L. I. Maissel[3] show a similar value for silicon dioxide. These results are somewhat

Table V

Sputtered Pyrex Coatings

Pressure Gauge (μHg)	Net RF Power (Watts)	Substrate Thermometer (°C)	Deposition Rate (μ/hr)	Approximate Gas Composition
0.54	355	200	0.26	Argon (Ar)
0.54	340	232	0.13	Ar then air
0.9	360	210	0.12	Air
0.5	380	180	0.24	Ar
1.0	350	130	0.05	O_2
1.0	360	150	0.15	60% Ar, 40% O_2
0.6	380	150	0.13	80% Ar, 20% O_2
0.6	390	170	0.10	Ar

Note:

4 to 5 mm thick pyrex plate used as target;

Electrode area: 79 cm^2.

surprising since an atom of tungsten can be sputtered with about one thousand electron volts of energy. Silver requires one-fifth as much energy as tungsten. Most of the 10 KeV per molecule required to sputter glass is dissipated at the target, converted to heat, and raises the temperature of the target. If it is assumed that the sputtering distribution from a point on the target follows the cosine pattern, then the geometrical factor in the material collection efficiency of the substrate is the same as the corresponding factor in the substrate's collection efficiency for heat radiated from the face of the target.

The collection efficiency of sputtered material per unit area of the substrate will be affected by two factors. The first factor (G) is due to geometry alone. The second factor is due to scattering of material molecules by ambient gas molecules. (Let U represent the fraction of molecules traveling toward the substrate which are unscattered before reaching the substrate.) This scattering is influenced by geometry and gas pressure. The fraction of sputtered molecules collected per unit area of the substrate is then G times U. (Each of these factors includes an elliptic integral of the space coordinates.)

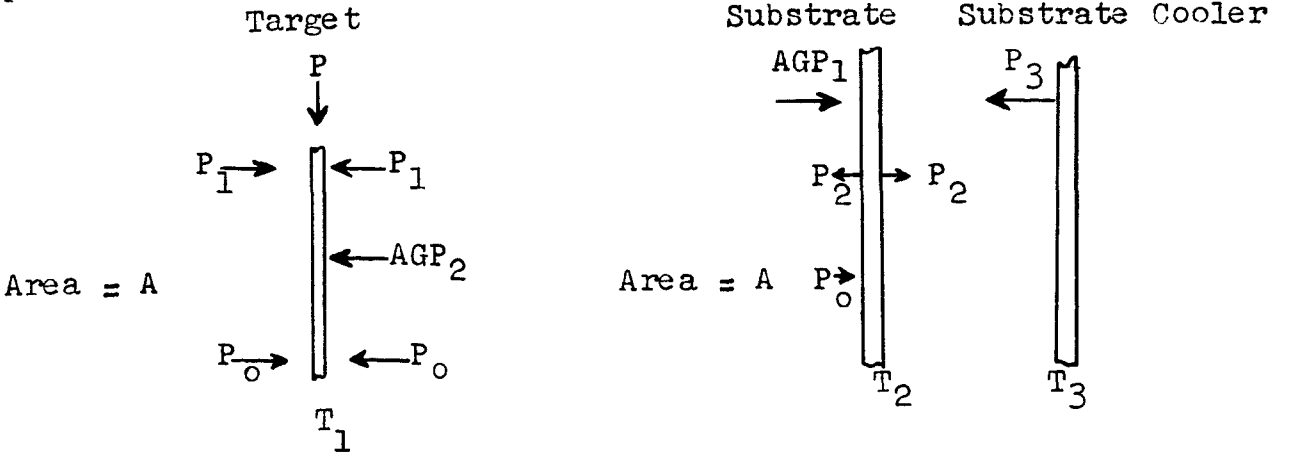

Assume that the sputtering target receives energy at a rate P from the bombarding ions. Assume also that it must radiate this to the chamber walls at a temperature T_o and to a substrate (assumed to have the same area A as the target). A fraction, G, of the power radiated from the face of the target is absorbed by a unit area of the face of the substrate. The substrate, in turn, radiates heat, half of which is absorbed by the substrate cooler and a fraction, AG, of which is absorbed by the face of the target. The substrate cooler is held at temperature T_3. Relations among T_o, T_1, T_2, T_3, and G are obtainable.

$$P = -2P_o + 2P_1 - AGP_2,\ P_o + AGP_1 + P_3 = 2P_2$$

$$P_o = A\sigma T_o^4,\ P_1 = A\sigma T_1^4,\ P_2 = A\sigma T_2^4,\ P_3 = A\sigma T_3^4$$

Then $P_1 = 1/2P + P_o + 1/2AGP_2$

If $A\sigma T_o^4 + 1/2AGP_2$ is negligble compared to P, $P_1 = 1/2P$

Then $T_1 = (p/2A\sigma)^{1/4}$

and $T_2 = (1/2T_o^4 + 1/2T_3^4 + 1/2GP/\sigma)^{1/4}$

also $G = 2\sigma(2T_2^4 - T_o^4 - T_3^4)/P$

R, the removal rate in mass per unit time for a given target at a given RF power is PQ, where Q is the number of grams removed per watt-second. The best Q we have achieved thus far is 7.5×10^{-8} gm/watt-second, at a power density of 5.0 watts/cm^2.

The deposition rate is RGU which may be rewritten $2Q\sigma U(2T_2^4 - T_o^4)$ in mass per unit area per unit time or

$r = 2Q\sigma U(2T_2^4 - T_o^4 - T_3^4)/\rho$ in thickness per unit time. This can be solved for the substrate temperature,

$$T_2 = (1/2)^{1/4} (T_o^4 + T_3^4 + r\ \rho/Q\sigma U)^{1/4}$$

$$\sigma = 5.679 \times 10^{-12} \text{ watt/cm°K}^4.$$

Figure 7 shows substrate temperature as a function of deposition rate for three different values of the unscattered fraction assuming $\rho = 2.4$ gm/cm^3 and $T_o = T_3 = 290°K$.

Measurements

The properties of films were determined by measurement of thickness, emittance, reflectance, cell spectral response, effects of humidity, dessicated air, and vacuum.

1. Thickness

The thickness of deposited films can be measured in several ways: multiple beam interferometry, shallow field microscope, or measurement of weight gain after deposition.

The shallow field microscope was used infrequently as the accuracy for measuring films less than 2-3 microns thick is poor. Subsequently, all the initial thickness measurements were accomplished by measurement of weight before and after deposition. These measurements were correlated with the multiple beam interferometer. Agreement between the last two methods was quite good with the error probably less than 150 Å out of 10,000 Å. The multiple beam interferometer necessitates deposition of an opaque, highly reflecting film over the coating itself. Consequently, the films on cells were measured using the weight gain method. This was more than satisfactory for

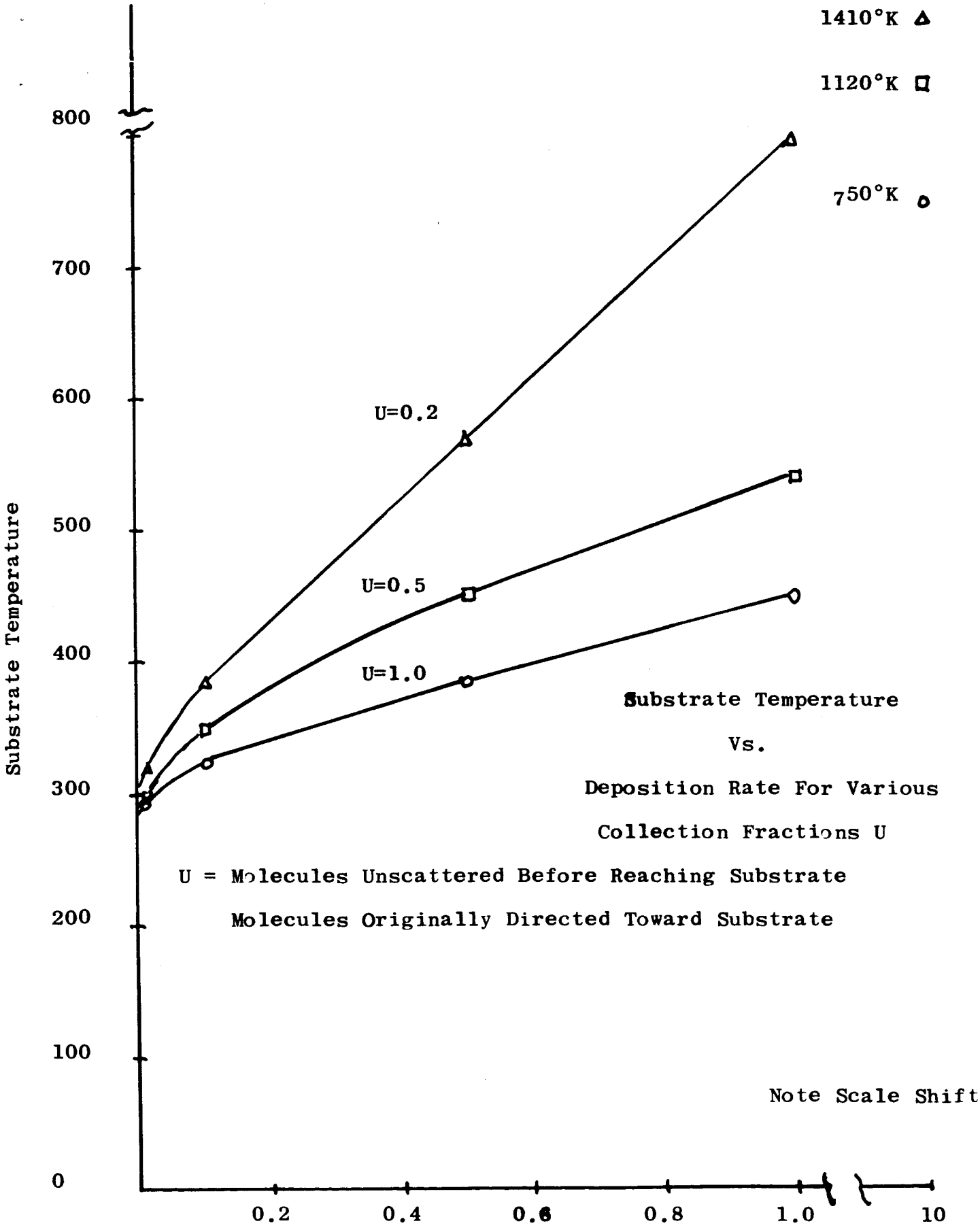
1410°K
1120°K
750°K
800
700
600
500
400
300
200
100
0
Substrate Temperature
U=0.2
U=0.5
U=1.0
Substrate Temperature
Vs.
Deposition Rate For Various
Collection Fractions U
U = Molecules Unscattered Before Reaching Substrate
Molecules Originally Directed Toward Substrate
Note Scale Shift
0.2
0.4
0.6
0.8
1.0
10
Deposition Rate In Microns Per Hour

Figure 7

for our purposes.

2. Reflectance

One of the important features of the optical coating of the CdS cell is the film's emittance at 9-10 microns, the peak in the radiant emittance curve of a 300°K black body. This emittance can be deduced from measurement of total reflectance. The equipment used were General Electric and Perkin-Elmer spectrophotometers. The GE unit, equipped with an integrating sphere, is capable of measuring total reflectance in the range from .3 to .7 microns. The Perkin-Elmer spectrophotometer measured specular reflectance in the range from 2.5 to 30 microns. Since the sample surfaces are not specular in nature, Rayleigh scattering is a major factor in determining the functional dependence of specular reflectance on wavelength. In order to determine the total reflectance of the coating, it was necessary to coat one-half of the sample surface with about 1000 Å aluminum. The specular reflectance of the two surfaces were determined and the total reflectance was found by taking the ratio of the specular reflectance of the coating to the specular reflectance of the coating with the aluminum overlay. Figure 8 shows the specular reflectance of a typical cell coated with sputtered pyrex glass. The interference pattern of the CdS on molybdenum can be seen along with evidence of Rayleigh scattering. The CdS film thickness can also be calculated from the curve

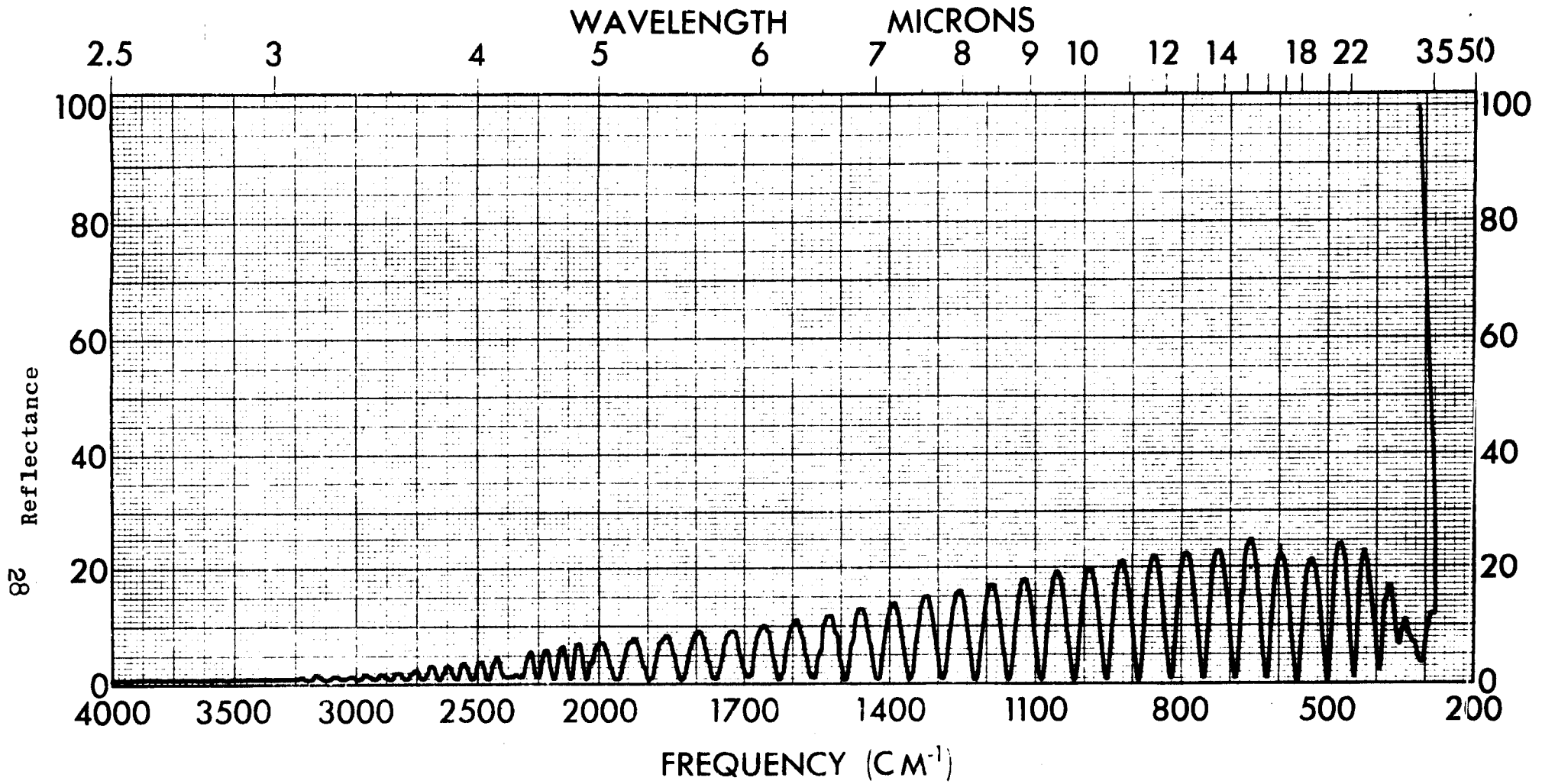

Spectrum No. G-1489 Phase: Solid

Sample: CdS Cell Date: 6-7-65

Origin: AN 64198 Remarks: Specular Reflectance Spectrum

Reflectance of CdS Cell Coated With Pyrex Glass

Figure 8

as follows:

$$\text{Thickness} = \frac{N}{2(\mu - \sin^2 I)^{1/2}(V_1 - V_2)}$$

where N = number of maxima between V_1 and V_2

μ = refractive index

I = incidence angle = 13°

V_1, V_2 = wave numbers of extreme maxima in cm^{-1}

$$\text{thickness} = \frac{21}{2(2.5^2 - .22^2)^{1/2}(2000 - 600)}$$

= 30 microns

Figure 9 is the reflectance spectrum of a CdS cell with an opaque aluminum overlay. This curve is a good demonstration of Rayleigh scattering and the effect of particle size on the reflectance from the surface.

Figures 10, 11, and 12 are reflectance curves of thick crystals of MgF_2, CaF_2 and LiF respectively. The reflectance spectra of these are all satisfactory for the coating. All except MgF_2 were discarded after initial experiments, however, as unstable either mechanically, chemically, or in the van Allen radiation. Figure 13 is a typical reflectance curve of an uncoated CdS film. The interference pattern can be again noted. The CdS film when coated with MgF_2 and an opaque layer of evaporated aluminum is also an excellent example of Rayleigh scattering. This curve as shown in Figure 14 comes close to 100% reflectance at 20-30 microns whereas in Figure 15, the reflectance of the MgF_2 coated sample is sufficiently reduced. Comparison of Figures 14 and 15 will show that the coated sample has a reflectance of about 30%. This would lead to an emittance of 70% which is sufficient.

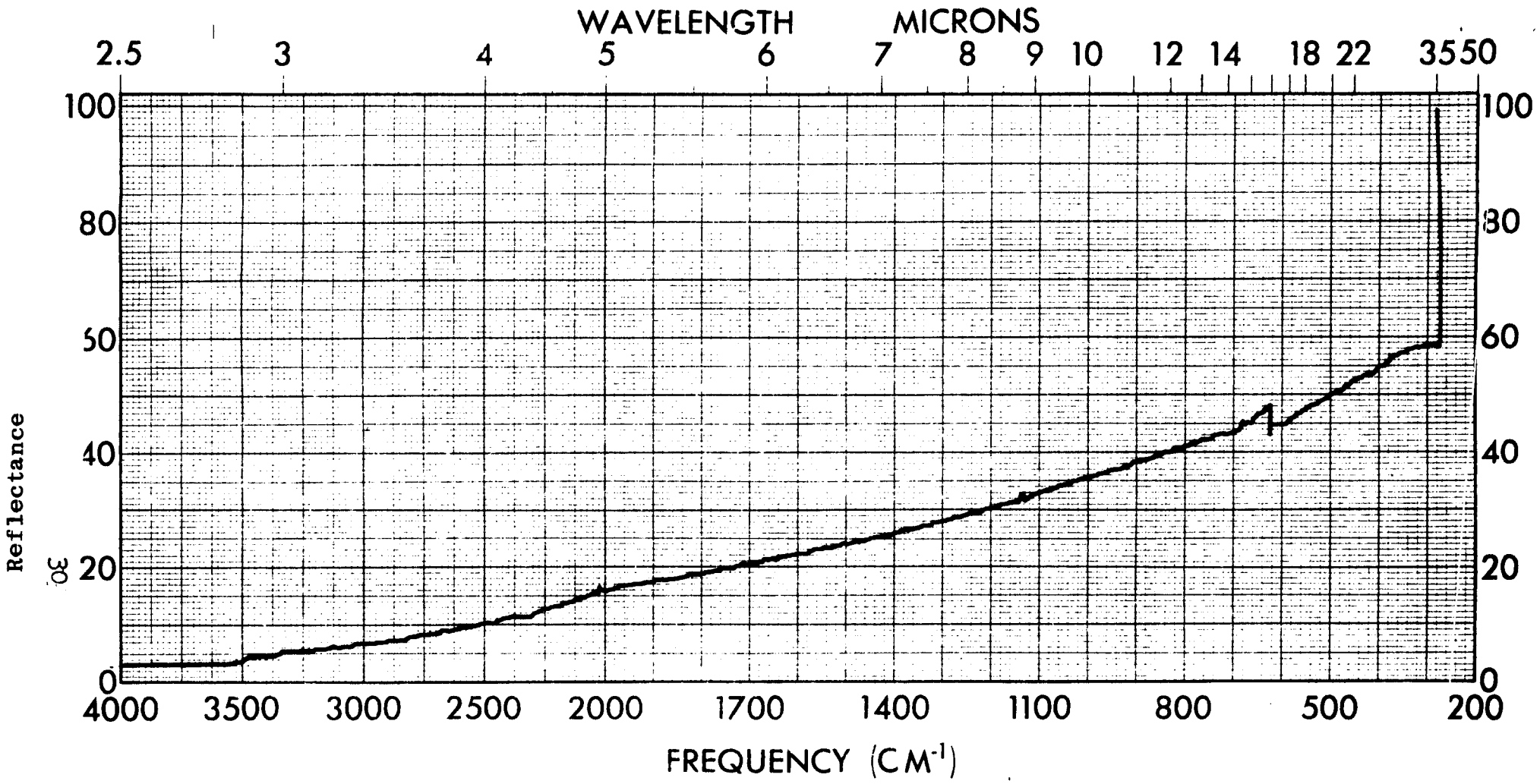

Spectrum No. G-1487 Phase: Solid

Sample: Al on CdS Cell Date: 6-7-65

Origin: AN 64198 Remarks: Specular Reflectance Spectrum

Reflectance of Aluminum on CdS Cell No. M526

Figure 9

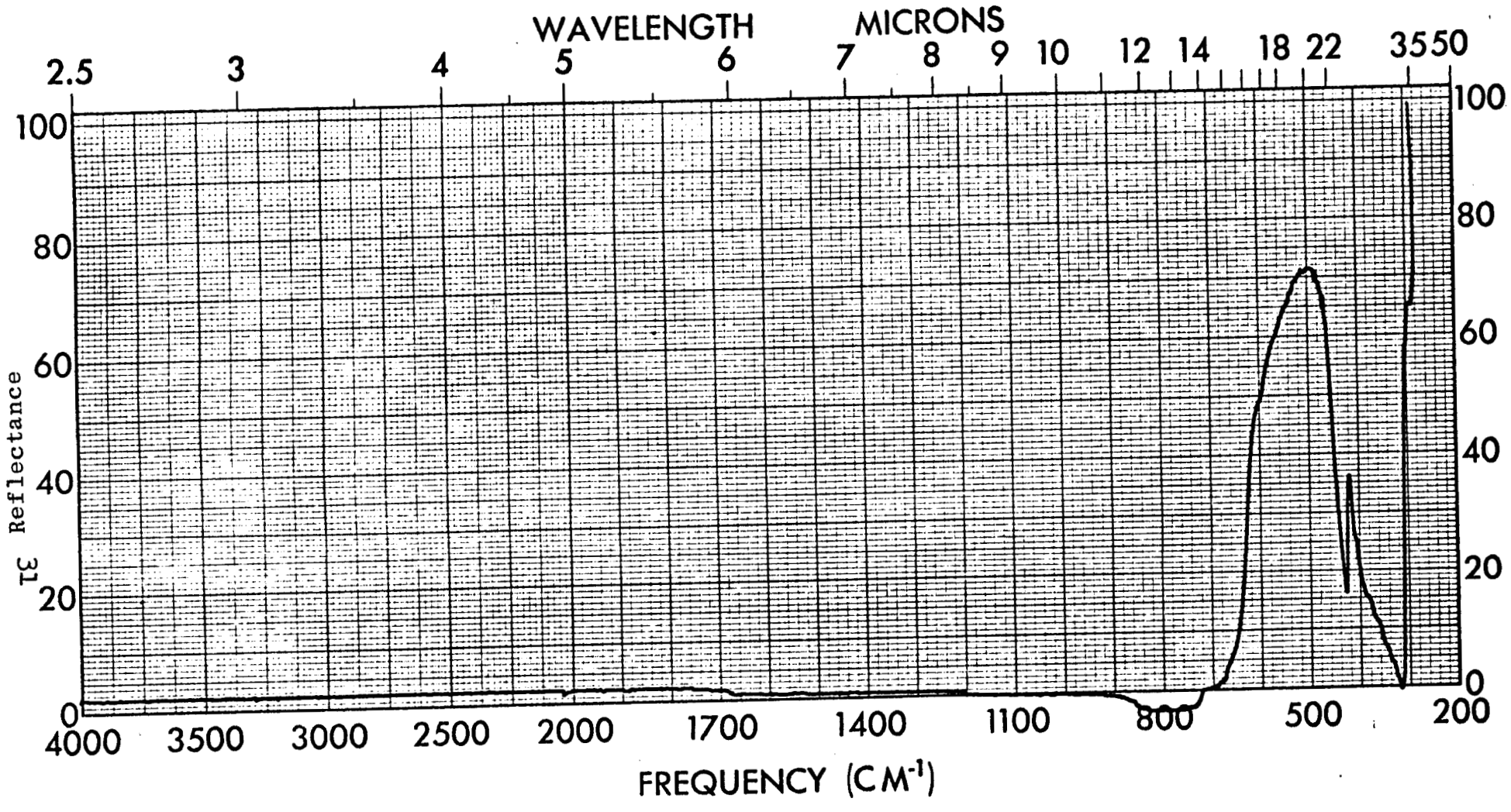

Spectrum No. G-1961 Phase: Solid

Sample: MgF_2 Cell Date: 10-28-65

Origin: AN 64198 Remarks: Specular Reflectance Spectrum

Reflectance of MgF_2 Crystal

Figure 10

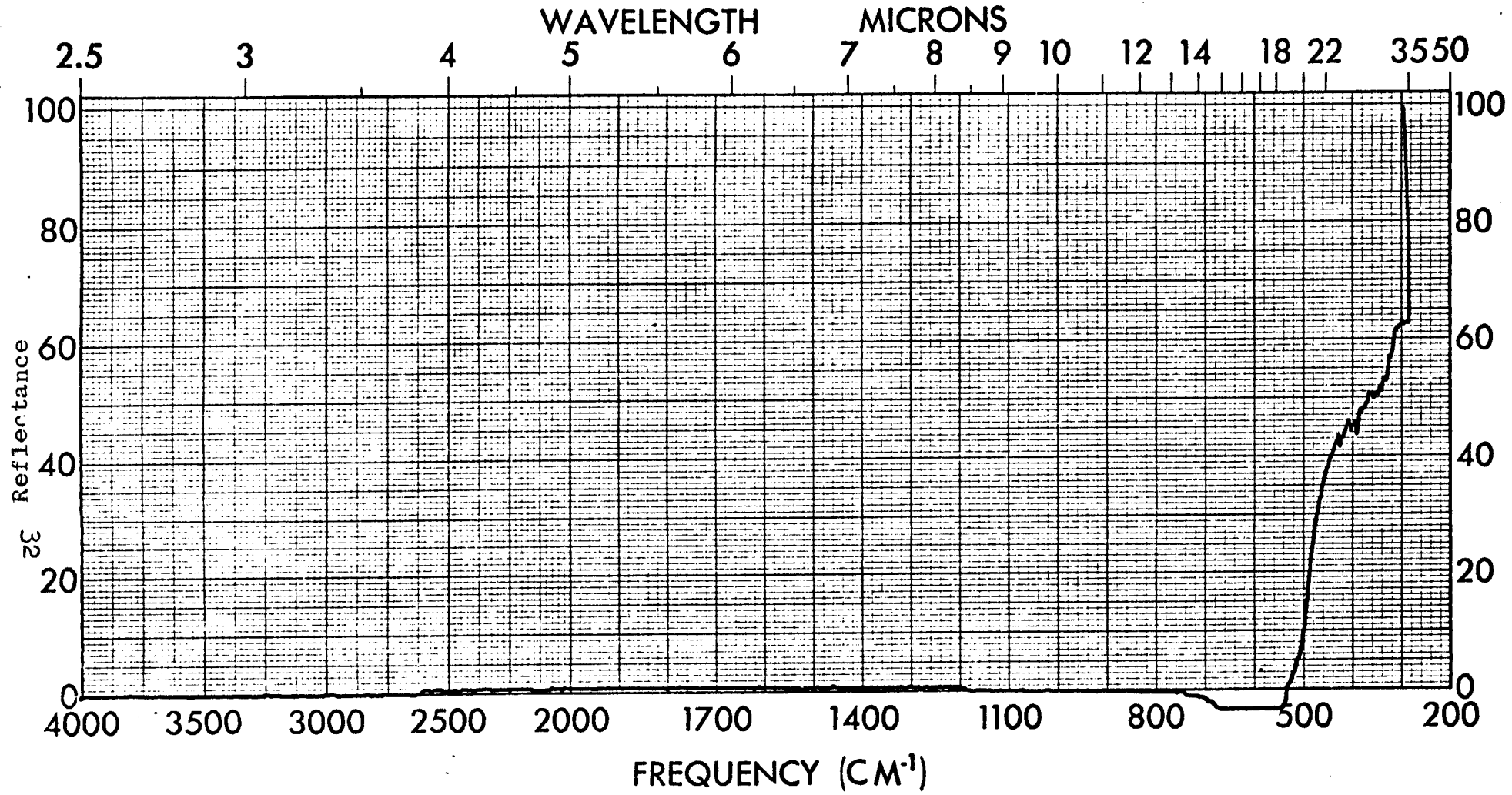

Spectrum No. G-1962 Phase: Solid

Sample: CaF_2 Date: 10-28-65

Origin: An 64198 Remarks: Specular Reflectance Spectrum

Reflectance of CaF_2 Crystal

Figure 11

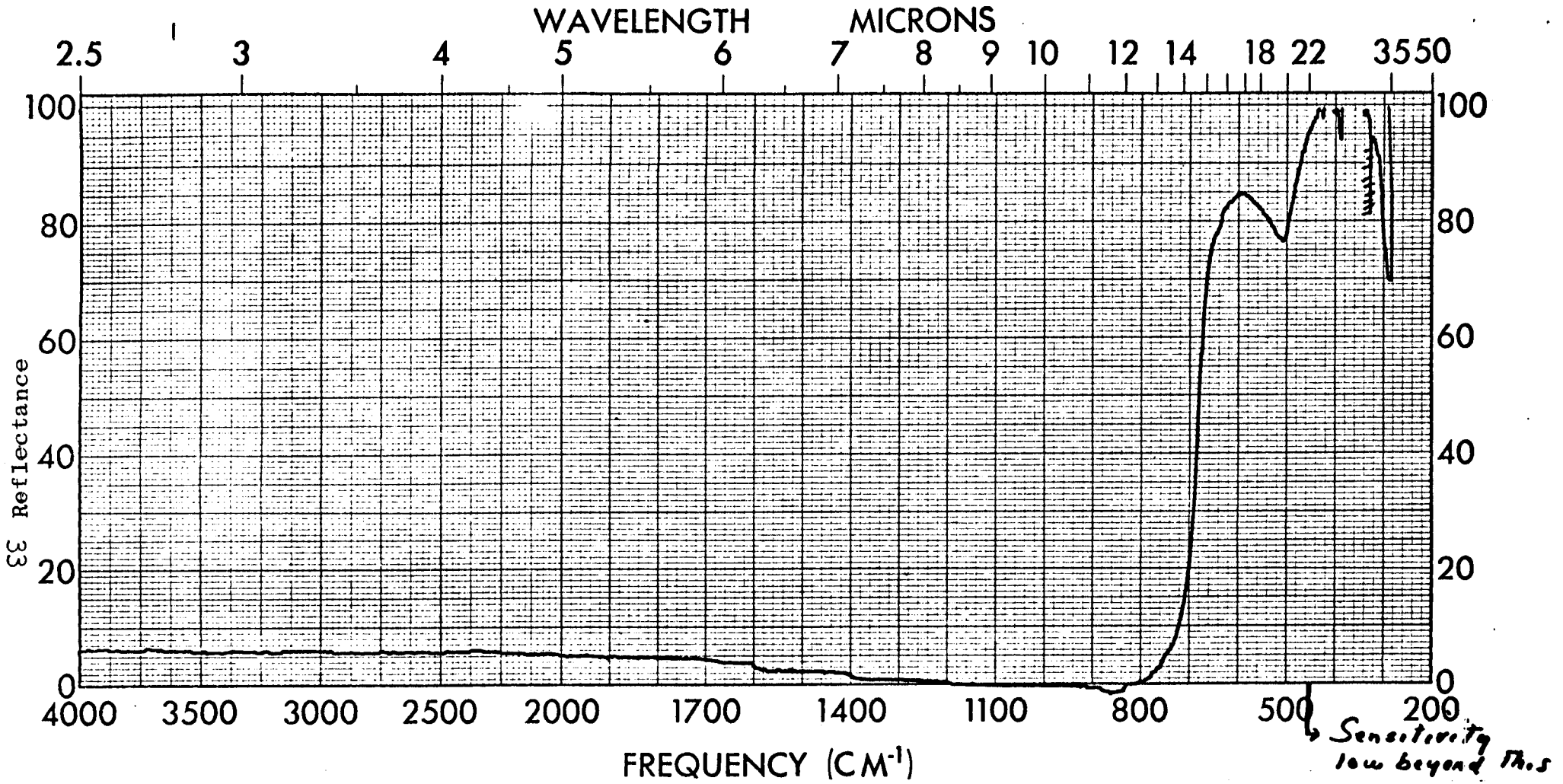

Spectrum No. G-1960 Phase: Solid

Sample: LiF Date: 10-28-65

Origin: An 64198 Remarks: Specular Reflectance Spectrum

Reflectance of LiF Crystal

Figure 12

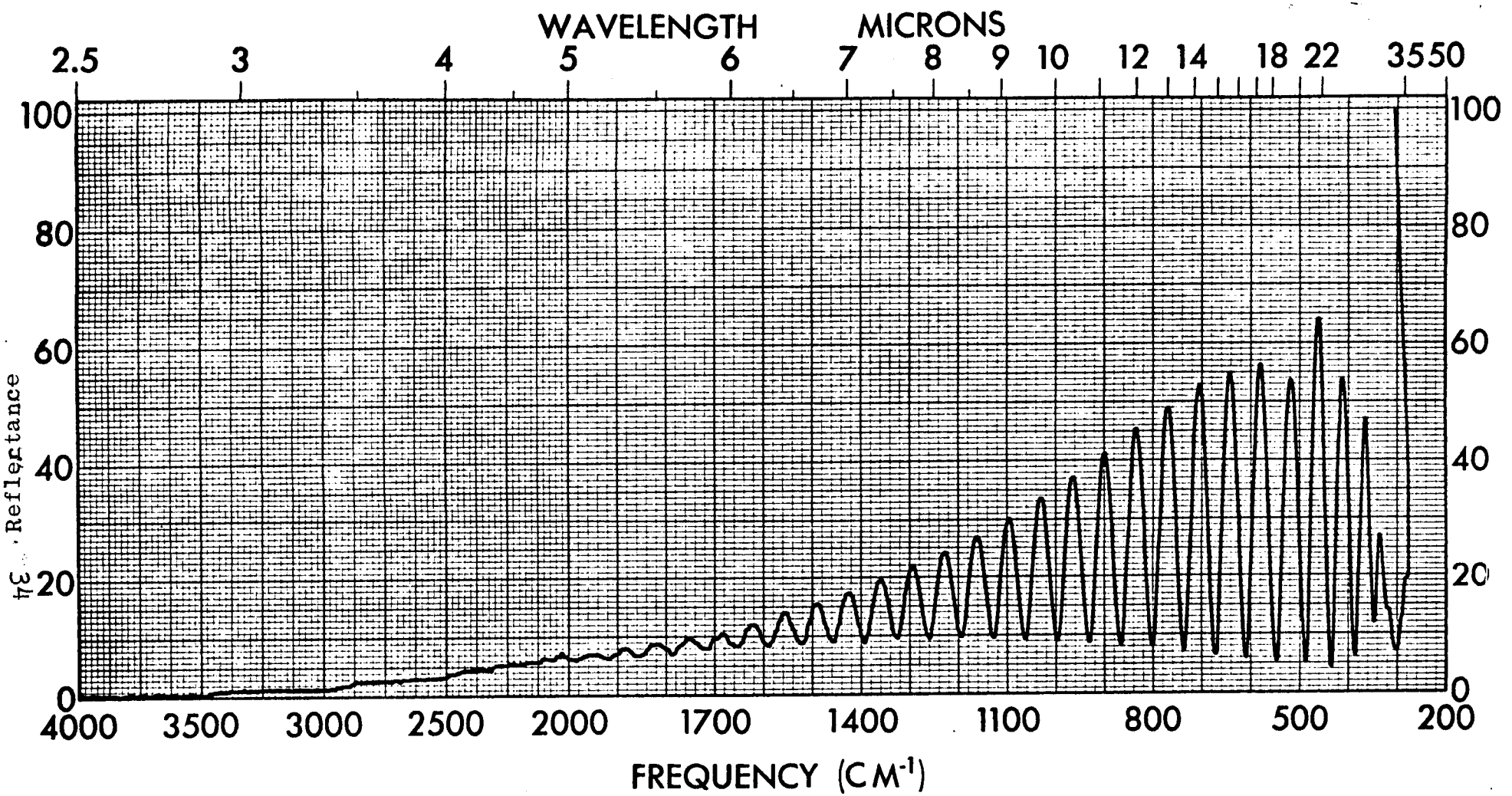

Spectrum No. G-1622 Phase: Solid

Sample: CdS Cell Date: 7-6-65

Origin: An 64198 Remarks: Specular Reflectance Spectrum

Reflectance of CdS Cell

Figure 13

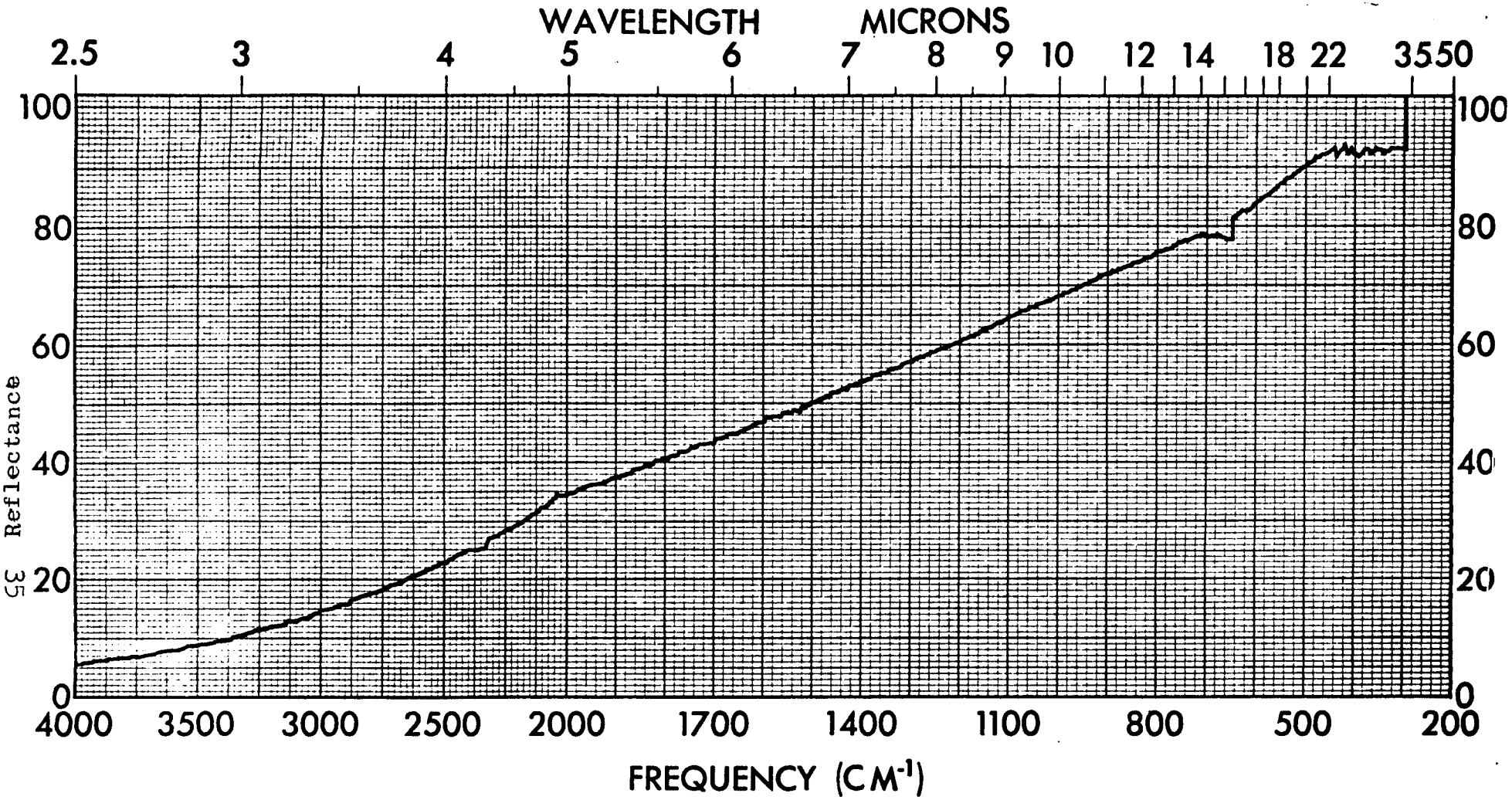

Spectrum No. G-1620 Phase: Solid

Sample: CdS Cell + Al + SiO_2 Date: 7-6-65

Origin: An 64198 Remarks: Specular Reflectance Spectrum

Reflectance of CdS Cell + Al + SiO_2

Figure 14

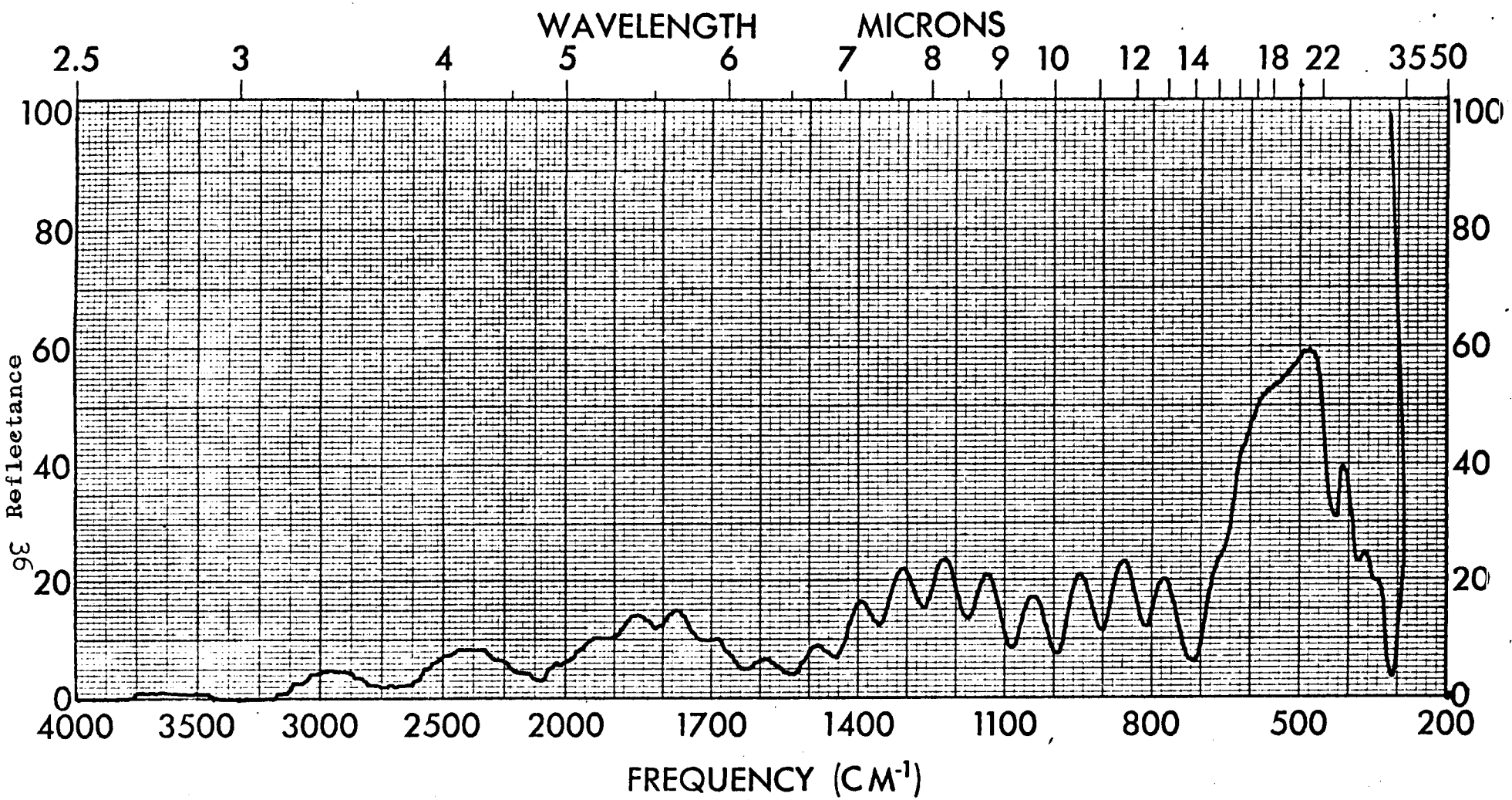

Spectrum No. G-1864 Phase: Solid

Sample: CdS Cell coated with MgF_2 (3 microns) Date: 10-5-65

Origin: An 65887 Remarks: Specular Reflectance Spectrum

Reflectance of CdS Cell + MgF_2 (3 microns thick)

Figure 15

3. Emittance

Spectral reflectance measurements provide an easy method of measuring emittance when the reflectance spectrum is simple in structure. However, the presence of absorption and reflection bands in the infrared complicate calculation of emittance at low temperatures. In this case, it is simpler to assembly a radiator from the material to be studied and measure its temperature at a known power dissipation. An apparatus was assembled to do this and it is shown schematically in Figures 16 and 17. A normal bell jar-vacuum set up was modified as follows. The interior of the bell jar and the baffle plate were coated with acetylene black to provide an isothermal room temperature enclosure with a high emissivity. A flat heater was made from small diameter copper magnet wire with Al_2O_3 plates bonded to each side of the heater, and suspended vertically in the approximate center of the bell jar. Since the resistance of the heater is proportional to the temperature, measurement of current and voltage is an accurate indication of the temperature of the heater and/or the sample surface. The heater surfaces (Al_2O_3) were blackened with acetylene black in order to have the same emittance and reflectance as the interior of the chamber. At a steady state condition the thermal equation of the system is:

$$P = P_1 + P_o$$

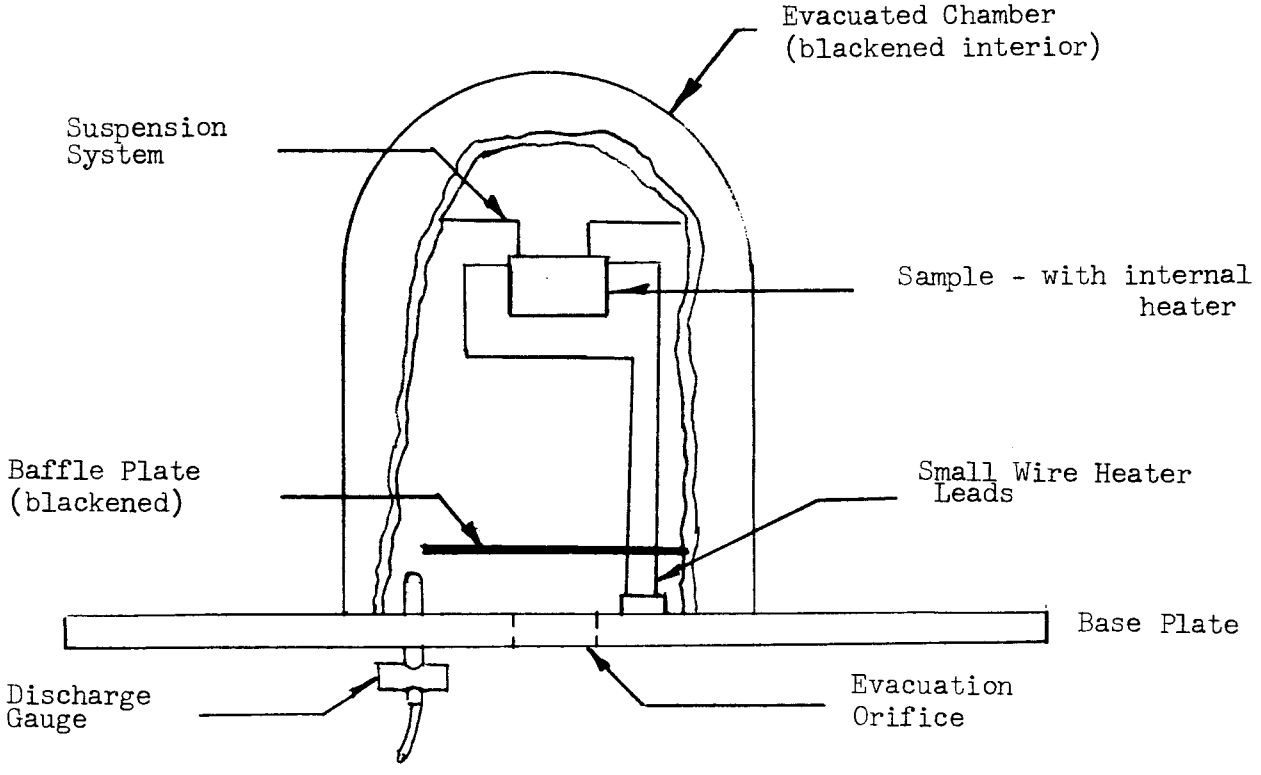

Figure 16 Emittance Measurement Apparatus

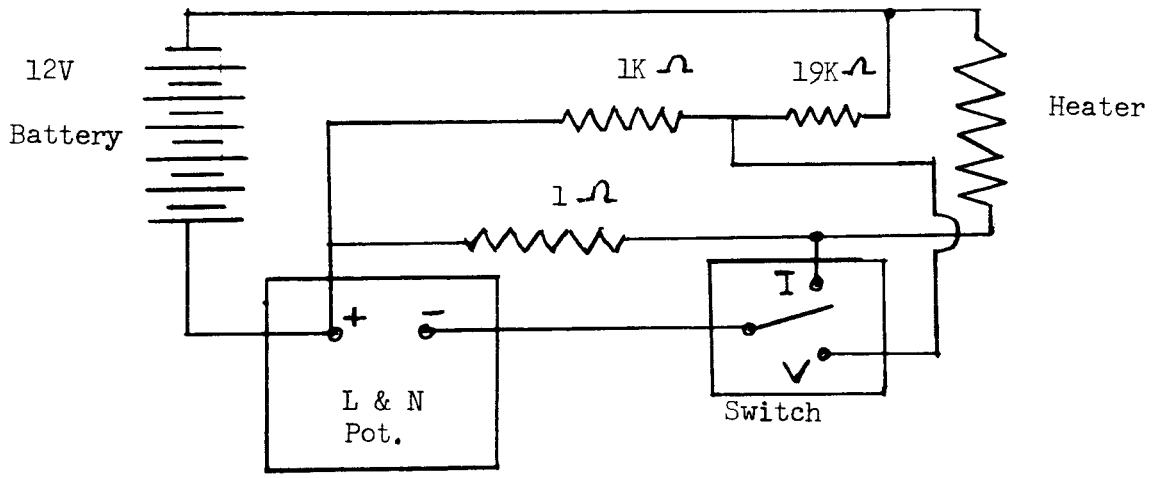

Figure 17 Measuring Circuit - Power & Temperature

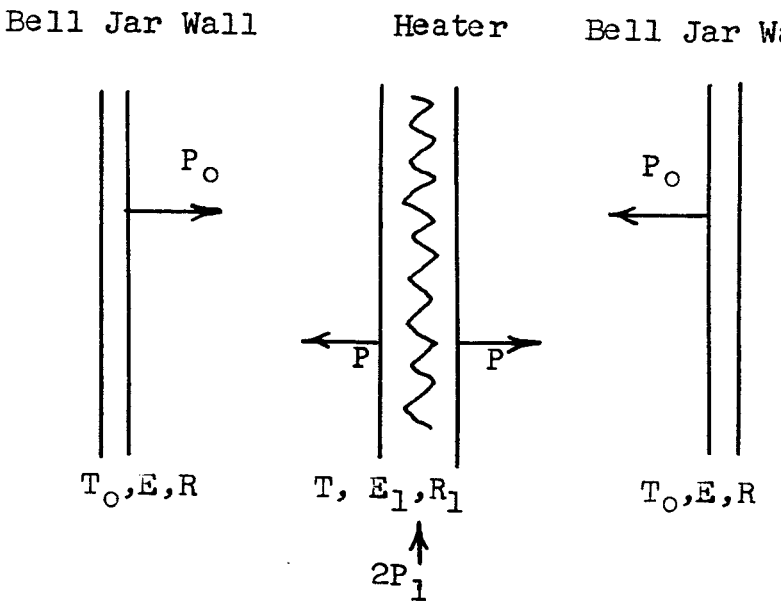

$$P = P_1 + P_o$$

where: P = Power radiated from sample + Power reflected from sample of wall radiation + Power reflected from sample of wall reflection of sample radiation.

P_o = Power radiated from wall + Power reflected from wall of sample radiation + Power reflected from wall of sample reflection of wall radiation.

P_1 = Electrical power into heater considering only one side of sample surface.

Evaluating the above produces the following equations:

$$P = E_1\sigma AT^4 + R_1P_o' \ (1 + R_1R + R_1{}^2R^2 + ...)$$
$$+ RR_1P' \ (1 + R_1R + R_1{}^2R^2 + ...)$$
$$P_o = E\sigma AT_o{}^4 + RP' \ (1 + R_1R + R_1{}^2R^2 + ...)$$
$$+ R_1RP_o{}^1(1 + R_1R + R_1{}^2R^2 + ...)$$

Let $P_0' = E\sigma AT_0^4$ and

$P' = E_1\sigma AT^4$

Substituting in:

$$P_1 + P_0 = P$$

Produces:

$$P_1 + \left(1 + \frac{R_1R}{1 - R_1R}\right) E\sigma AT_0^4 + \frac{R}{1 - R_1R} E_1\sigma AT^4$$

$$1 + \frac{R_1R}{1-R_1R} E_1\sigma AT^4 + \frac{R_1}{1 - R_1R} E\sigma AT_0^4$$

where: $1 + R_1R + R_1^2R^2 + R_1^3R^3 + \ldots\ldots = \frac{1}{1 - R_1R}$

and allowing:

$$R = 1 - E$$

$$R_1 = 1 - E_1$$

$$R_1R = 1 - E - E_1 + E_1E$$

gives:

$$E_1 = \frac{\frac{P_1}{\sigma A}}{T^4 - T_0^4 + \frac{P_1}{\sigma A}\left(1 - \frac{1}{E}\right)}$$

where: E = emissivity of acetylene black = .93

σ = 5.67×10^{-12} watts/cm^2 °K^4

A = area of heater (one side)

T_0 = wall temperature

T = sample temperature

and E_1 = the emittance of the sample coating

The emittance of acetylene black was determined by setting $E_1 = E$ in the above equation. Several coating materials were measured for emittance using the above set-up. Correlation between published values and calculated values were in quite close agreement showing the validity of the measurement. Table VI lists some of our findings and those published for particular materials.

4. Humidity & Vacuum

While the primary purpose of this program was oriented towards an optical coating for CdS cells, it was hoped that the cell would be stable when exposed to ambient high humidities. Unfortunately, this was not accomplished. A series of tests were made of cells that were coated with MgF_2 and SiO-MgF_2, uncoated cells, and cells laminated in a plastic sandwich.

The results were not promising. Figures 18, 19, and 20 show the rapid degradation of almost all cells after exposure to 90% RH. The best results obtained were on the cells that had been laminated. After examination of the coated cells under magnification and before exposure to high humidity, it was noted that the coating was discontinuous. Uncoated, coated and laminated cells were also stored in vacuum for observation of the cell behavior over a period of time. All three types of cells had more or less the same type of stabilization curve as can be seen in Figure 21. At the various check points of time versus output, the cells were also observed as regard to spectral response characteristics. This was accomplished by the placing of optical filters with different cut-off points

Table VI

EMITTANCE

Material Tested	Calculated E	Published Values E
Acetylene Black	.93	.95
CdS Cell Uncoated	.22	
Glass	.86	.90
Silicone Primer		
GE-SS-4044	.26	
Aluminum	.02 - .04	.03
CdS Cell Coated with Silicone Primer	.26	
MgO	.09	.15
Aluminum Coated with MgF_2	.22	
CdS Cell Coated with MgF_2	.70	

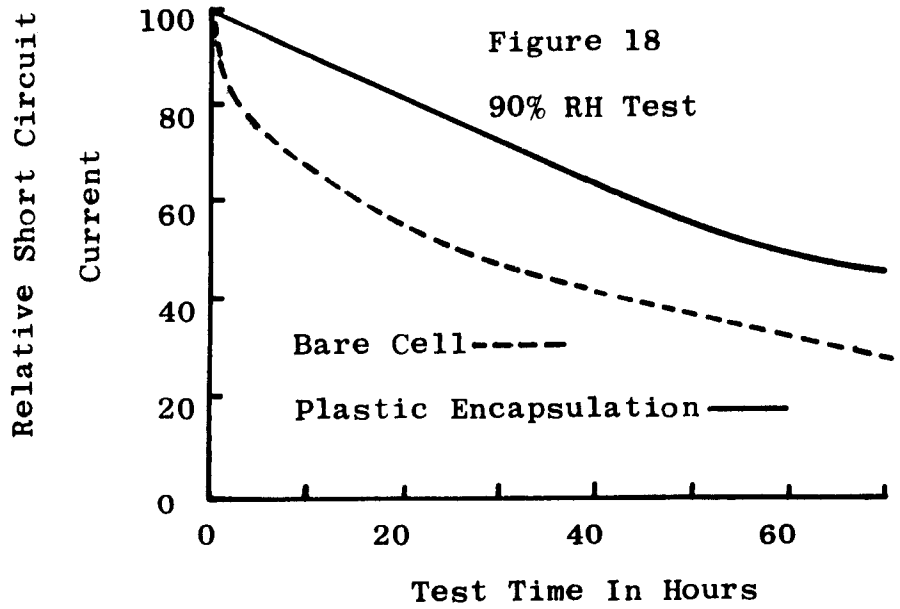

Figure 18

90% RH Test

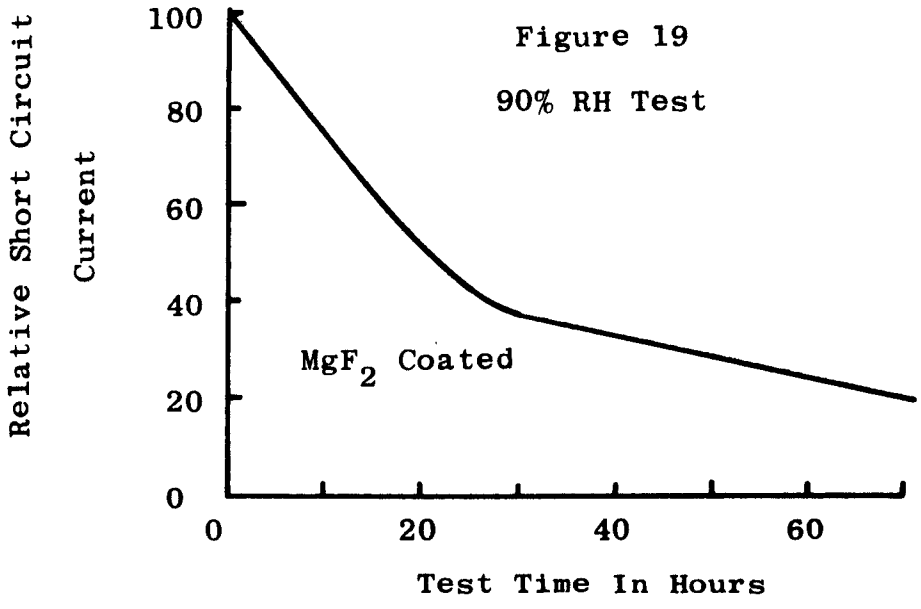

Figure 19

90% RH Test

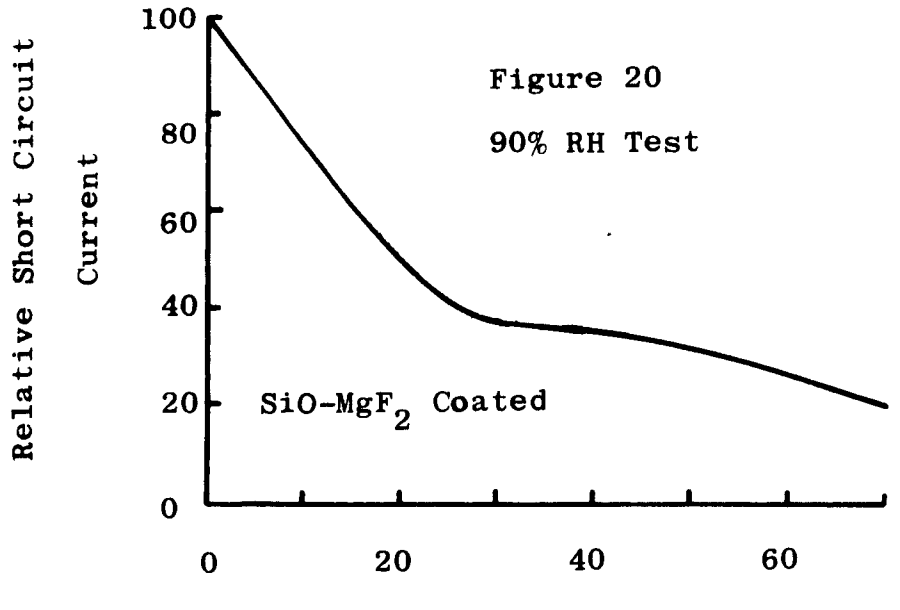

Figure 20

90% RH Test

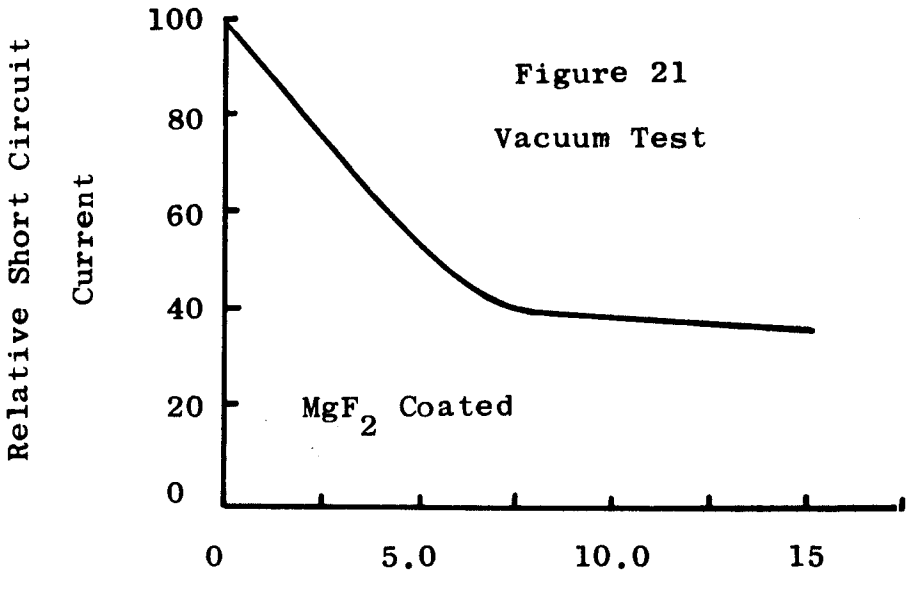

Figure 21

Vacuum Test

between the light source and the CdS cell. This could be considered as a selective spectral response check. No particular differences were noted in the degradation curves of the various type cells regardless of the coating or cover material.

Conclusions

As a result of the work done on this program, it is concluded that deposition of dielectric films onto CdS solar cells by sputtering is not feasible. In addition to the inherent instabilities in the system at the necessary power levels, the temperature rise of the substrate cell is intolerable at the required deposition rates. While there may be ways to avoid these problems, the resulting complexity of the system would appear to render it impractical.

The vacuum thermal evaporation of MgF_2 on the other hand is simple and produces films with the necessary optical properties. The heavy MgF_2 layers do not seem to be suitable moisture barriers, but in conjunction with an underlayer of 3000 Å of SiO should be adequate. It is felt that the plastic overlayer will not provide either moisture protection or a sufficiently highly emitting surface. While the MgF_2 films were mechanically imperfect, it is reasonable to expect that a suitable combination of deposition rate and substrate temperature can eliminate this problem.

References

(1) "Introduction to Solid State Physics", C. Kittel, 2nd Edition, John Wiley and Sons, pp.112-116

(2) G. Anderson, W. Mayer, G. Wehner, J., Appl. Phys., 33, 2991 (1962)

(3) RF Sputtering - "Yield Studies for Various Materials," P. D. Davidse and L. I. Maissel. This paper was delivered at the Thin Film Division Symposium of the 12th National Vacuum Symposium of the American Vacuum Society on September 30, 1965.

Harshaw Chemical Company
Contract NAS3-6464

Quarterly Reports

DISTRIBUTION LIST

	No. of Copies
National Aeronautics and Space Administration Washington, D. C. 20546 Attention: Arvin H. Smith/RNW	2
National Aeronautics and Space Administration Washington, D. C. 20546 Attention: H. B. Finger/RP	1
National Aeronautics and Space Administration Washington, D. C. 20546 Attention: Millie Ruda/AFSS-LD	1
National Aeronautics and Space Administration Scientific and Technical Information Facility P. O. Box 5700 Bethesda, Maryland 20546 Attention: NASA Representative	5 + 1 repro.
National Aeronautics and Space Administration Goddard Space Flight Center Greenbelt, Maryland 20771	
Attention: W. R. Cherry	1
Attention: M. Schach	1
Attention: B. Mermelstein, Code 672	1
Attention: J. W. Callaghan, Code 621	1
Attention: Librarian	1
Attention: P. H. Fang, Code 633	5
National Aeronautics and Space Administration Lewis Research Center 21000 Brookpark Road Cleveland, Ohio 44135	
Attention: John E. Dilley, MS 500-309	1
Attention: B. Lubarsky, MS 500-201	1
Attention: H. Shumaker, MS 500-201	1
Attention: R. L. Cummings, MS 500-201	1
Attention: C. K. Swartz, MS 500-201	3 + 1 repro.
Attention: N. D. Sanders, MS 302-1	1
Attention: Dr. A. E. Potter, MS 302-1	3
Attention: C. S. Corcoran, MS 500-201	1

	No. of Copies
Attention: George Mandel, MS 5-1	2
Attention: Report Control Office	1
Attention: Technology Utilization Office, MS 3-16	1
National Aeronautics and Space Administration Langley Research Center Langley Station Hampton, Virginia 23365	
Attention: W. C. Hulton	1
Attention: E. Rind	1
Jet Propulsion Laboratory 4800 Oak Grove Drive Pasadena, California 91103	
Attention: John V. Goldsmith	1
Attention: Don W. Ritchie	1
Institute for Defense Analysis Connecticut Avenue, N.W. Washington, D. C. 20546	
Attention: R. Hamilton	1
Advanced Research Projects Agency Department of Defense, Pentagon Washington, D. C. 20546	
Attention: Dr. C. Yost	1
Naval Research Laboratory Department of the Navy Washington, D. C. 20546	
Attention: E. Broncato, Code 6464	1
Attention: M. Wotaw, Code 5170	1
Attention: Dr. V. Linnenbom, Code 7450	1
Attention: Dr. C. Klick, Code 6440	1
U. S. Army Signal Research and Development Laboratory Fort Monmouth, New Jersey	
Attention: Power Sources Branch	1
Air Force Cambridge Research Center Air Research and Development Command United States Air Force Laurence G. Hanscom Field Bedford, Massachusetts	
Attention: Col. G. de Giacomo	1

	No. of Copies
Air Force Ballistic Missile Division Air Force Unit Post Office Los Angeles 45, California	
Attention: Col. L. Norman, SSEM	1
Attention: Lt. Col. G. Austin, SSZAS	1
Attention: Lt. Col. A. Bush, SSZME	1
Attention: Capt. A. Johnson, SSZDT	1
Attention: Capt. W. Hoover, SSTRE	1
Office of the Chief of Engineers Technical Development Branch Washington, D. C.	
Attention: James E. Melcoln/ENGMC-ED	1
Aeronautical Research Laboratories Office of Aerospace Research, USAF Wright-Patterson Air Force Base Dayton, Ohio	
Attention: Mr. D. C. Reynolds, ARX Chief, Solid State Physics, Research Lab.	1
Aeronautical Systems Division Air Force Systems Command United States Air Force Wright-Patterson Air Force Base, Ohio	
Attention: P. R. Betheand	1
Attention: Mrs. E. Tarrants/WWRNEM-1	1
Flight Vehicle Power Branch Air Force Aero Propulsion Laboratory Wright-Patterson Air Force Base, Ohio	
Attention: Joe Wise/Code APIP-2	1
Flight Accessories Aeronautics Systems Division Wright-Patterson Air Force Base Dayton, Ohio	
Attention: James L. Matice, ASRCN-22	1
Aerospace Corporation P. O. Box 95085 Los Angeles 45, California	
Attention: Dr. G. Hove	1
Attention: Dr. F. Mozer	1
Attention: V. J. Porfune	1
Attention: Dr. I. Spiro	1
Attention: Technical Library Documents Group	1

	No. of Copies
Battelle Memorial Institute 505 King Avenue Columbus, Ohio	
Attention: L. W. Aukerman	1
Attention: R. E. Bowman	1
Attention: T. Shielladay	1
Bell and Howell Research Center 360 Sierre Madre Villa Pasadena, California	
Attention: Alan G. Richards	1
Bell Telephone Laboratories, Incorporated Murray Hill, New Jersey	
Attention: W. L. Brown	1
Attention: U. B. Thomas	1
Clevite Corporation Electronic Research Division 540 East 105th Street Cleveland 8, Ohio	
Attention: Fred A. Shirland	1
Attention: Dr. Hans Jaffe	1
The Eagle-Picher Company Chemical and Material Division Miami Research Laboratories 200 Ninth Avenue, N. E. Miami, Oklahoma	
Attention: John R. Musgrave	1
Energy Conversion, Incorporated 336 Main Street Cambridge 42, Massachusetts	
Attention: G. J. McCaul	1
General Electric Company Electric Components Division 316 East Nineth Street Owensboro, Kentucky	
Attention: F. D. Dyer, Jr.	1
Heliotek Corporation 12500 Gladstone Avenue Sylmar, California	
Attention: Eugene Ralph	1

	No. of Copies
Hughes Aircraft Company Aerospace Group, R&D Division Culver City, California Attention: C. A. Escoffery	1
International Rectifier Corporation 239 Kansas Street El Segundo, California Attention: Irwin Rubin	1
Leesona Moos Laboratories 90-28 Van Wyck Expressway Jamaica 18, New York Attention: Stanley Wallack	1
Material Research Corporation Orangeburg, New York 10962 Attention: Vernon E. Adler	1
Martin Company Orlando, Florida Attention: W. A. Headley, Jr.	1
National Cash Register Company Physical Research Department Dayton 9, Ohio Attention: R. R. Chamberlin	1
North American Aviation, Incorporated Autonetics Division Anaheim, California Attention: R. R. August	1
Perkin-Elmer Company Optical Coating Section Norwalk, Connecticut Attention: Jim Beardsley	1
Philco Corporation Blue Bell, Pennsylvania Attention: Mr. A. E. Mace	1
RCA Laboratories Radio Corporation of America Princeton, New Jersey Attention: P. Rappaport	1

	No. of Copies
Sandia Corporation Albuquerque, New Mexico Attention: F. Smits	1
Sylvania Electronic Products, Incorporated Electron Tube Division Emporium, Pennsylvania Attention: Georgiana Larrabee, Librarian	1
Union Carbide Corporation Parma Research Center Technical Information Services P. O. Box 6116 Cleveland, Ohio 44101	1
Solid-State Electronics Laboratory Stanford Electronics Laboratories Stanford University Stanford, California Attention: Prof. G. L. Pearson	1
Westinghouse Electric Corporation Research and Development Laboratories Churchill Borough, Pennsylvania Attention: H. G. Chang	1
Westinghouse Electric Corporation Semiconductor Division Youngwood, Pennsylvania Attention: Don Gunther	1
Massachusetts Institute of Technology Security Records Office Room 14-0641 Cambridge 39, Massachusetts	1

Added

Lockheed Missiles & Space Company Technical Information Center 3251 Hanover Street Palo Alto, California	